Important note:

This technical report has been split into two sections to reduce file size for download. This document, part two, represents the accompanying figures for *Sand dune processes and management for flood and coastal defence Part 5: Dune management practices and options at selected dune systems in England and Wales.*

The main text of the report can be found in part one.

Tables

Table 5.1 Comparison of controlling environmental variables at the five study sites.

	Sefton	Kenfig	Studland	Brancaster	Spurn
Wind/wave climate	moderate	moderate-high	low-moderate	low-moderate	moderate-high
Tidal range (m)	macro-tidal	macro-tidal	micro-tidal	macro-tidal	macro-tidal
Beach sediment characteristics	sand	sand-pebbles	sand	sand	sand-pebbles
Sediment supply	moderate	low	low	low	moderate

Table 5.2 Tidal levels and tidal ranges for the five sites, expressed in metres above Ordnance Datum Newlyn (ODN).

Site	HAT	MHWS	MHW	MHWN	MLWN	MLW	MLWS	LAT	MSTR	MTR
Sefton	5.20	4.07	3.22	2.37	-2.03	-2.98	-3.93	-4.93	8.00	6.20
Kenfig	5.60	4.60	3.40	2.20	-2.00	-3.15	-4.30	-5.30	8.90	6.55
Studland	1.20	0.80	0.55	0.30	-0.20	-0.50	-0.80	-1.40	1.60	1.05
Brancaster	4.00	2.73	2.22	1.72	-1.24	-2.00	-2.76	-3.75	5.49	4.22
Spurn	3.80	3.00	2.30	1.60	-1.20	-1.95	-2.70	-3.70	5.70	4.25

Data for Spurn (Spurn Head), Studland (Poole Harbour Entrance), Kenfig (Porthcawl) and Sefton (Formby) taken from Admiralty Tide Tables (Admiralty, 2001); for Brancaster from Halcrow (1988).

HAT – Highest Astronomical Tide
MHWS – Mean High Water Springs
MHW – Mean High Water
MHWN – Mean High Water Neaps
MLWN – Mean Low Water Neaps
MSL – Mean Low Water
MLWS – Mean Low Water Springs
LAT – Lowest Astronomical Tide
MSTR – Mean Spring Tidal Range
MTR – Mean Tidal Range

Table 5.3 Beach width and average slopes (between ODN and MHW) derived from lidar data (flown in 1998) and the corresponding erosion/accretion status of the frontal dunes between Hightown and Ainsdale. Transect positions are shown in Figure 5.10.

Transect	Erosion/accretion status of frontal dunes	Beach width (m)	Average beach slope (degrees)
60	Accreting	430	0.43
48	Transition	286	0.64
30	Eroding	216	0.85
26	Transition	584	0.32
20	Accreting	832	0.22

Table 5.4 Beach widths and average slopes (between ODN and MHW) derived from bathymetric charts (1949 and 2002) and the corresponding erosion/accretion status of the frontal dunes between Hightown and Formby. Transect positions are shown in Figure 5.10.

Transect	1949			2002		
	Erosion/accretion status of frontal dune	Beach width (m)	Average beach slope (degrees)	Erosion/accretion status of frontal dune	Beach width (m)	Average beach slope (degrees)
28	Eroding	540	0.35	Eroding	410	0.45
22	Eroding	200	0.90	Accreting	460	0.40
17	Accreting	640	0.30	Accreting	690	0.25

Table 5.5 Comparison of morphological parameters of the intertidal zone at the five study sites, derived from lidar data.

Morphological parameter		Sefton	Kenfig	Studland	Brancaster	Spurn
Beach width		Wide	Wide	Narrow	Moderate	Moderate
MLW–MHW (m)	Min	–	–	10	–	43
	Max	–	–	35	–	124
	Mean	–	–	18	–	86
	SD	–	–	8	–	25
	N	–	–	8	–	20
ODN–HAT (m)	Min	149	161	17	84	31
	Max	2131	205	70	375	81
	Mean	690	185	31	184	58
	SD	466	15	16	79	12
	N	59	9	12	22	21
ODN–MHW (m)	Min	129	113	5	35	21
	Max	1481	182	129	295	40
	Mean	475	152	17	133	24
	SD	287	19	34	66	4
	N	59	10	13	22	21
Beach slope		flat	moderate	steep	moderate	steep
MLW–MHW (degrees)	Min	–	–	1.7	–	2.0
	Max	–	–	6.0	–	5.6
	Mean	–	–	3.8	–	3.1
	SD	–	–	1.3	–	1.0
	N	–	–	8	–	20
ODN–MHW (degrees)	Min	0.1	1.1	0.2	0.4	3.3
	Max	1.4	1.7	6.7	3.6	6.3
	Mean	0.5	1.3	4.1	1.3	5.6
	SD	0.2	0.2	1.5	0.8	0.6
	N	59	10	13	22	21
ODN–HAT (degrees)	Min	0.1	1.6	1.0	0.6	2.7
	Max	2.0	2.0	4.1	2.7	7.1
	Mean	0.6	1.7	2.6	1.5	3.9
	SD	0.4	0.1	1.0	0.6	1.0
	N	59	9	12	22	21
MLWN-MHWN (degrees)	Min	0.3	0.9	2.9	0.3	1.8
	Max	0.5	1.1	5.7	1.2	6.5
	Mean	0.4	1.0	4.0	0.7	4.7
	SD	0.1	0.1	0.9	0.3	1.3
	N	5	8	10	11	21
MHWN-MHWS (degrees)	Min	0.1	1.8	0.6	0.4	1.6
	Max	8.4	5.3	5.3	7.2	7.2
	Mean	1.0	2.9	3.4	1.8	4.8
	SD	1.5	1.1	1.3	1.4	1.9
	N	70	10	13	22	21
Beach type (terminology of Short and Hesp, 1982)		Dissipative	Intermediate-dissipative	Intermediate-reflective	Intermediate	Intermediate-reflective

Table 5.6 Comparison of morphological parameters and features of the frontal dunes at the five study sites, derived from lidar data.

Morphological parameter		Sefton	Kenfig	Studland	Brancaster	Spurn
Frontal dune crest height (m ODN)	MIN	6.50	8.82	4.09	4.21	5.62
	MAX	18.90	16.13	6.51	12.15	13.80
	MEAN	10.52	12.04	4.97	6.67	8.66
	SD	3.14	2.65	0.86	2.23	2.27
	N	75	10	13	22	21
Frontal dune volume above HAT (m^3/m)	MIN	186	505	274	3	31
	MAX	1962	1389	582	544	927
	MEAN	822	762	428	143	254
	SD	366	268	93	176	256
	N	75	10	13	22	21
Frontal dune volume above ODN (m^3/m)	MIN	1227	1633	518	593	389
	MAX	3022	2510	826	1335	1688
	MEAN	1866	1887	670	851	801
	SD	369	266	94	234	369
	N	75	10	13	22	21
Dune types		Foredune ridges Transgressive dune sheets (Formby Point) Parabolic dunes, blowouts (Formby Point) Hummock dunes (Formby Point) Embryonic dunes (north and south) Beach ridges (north)	Single foredune ridge Parabolic dunes, blowouts Hummock dunes	Low multiple foredune ridges	Single foredune ridge (centre) Recurves (notably in the east)	Multiple foredune ridges (more ridges in the south) Embryonic dunes (mainly in the south)

Figures

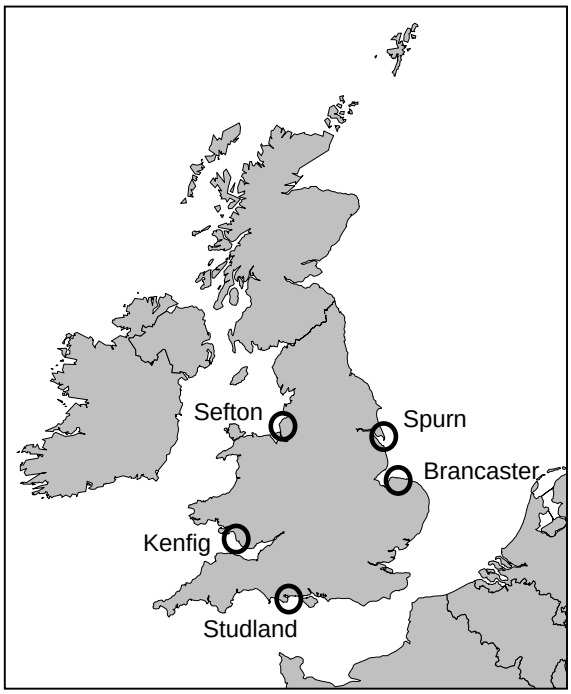

Figure 5.1 Location of the five dune sites considered as case studies in this report.

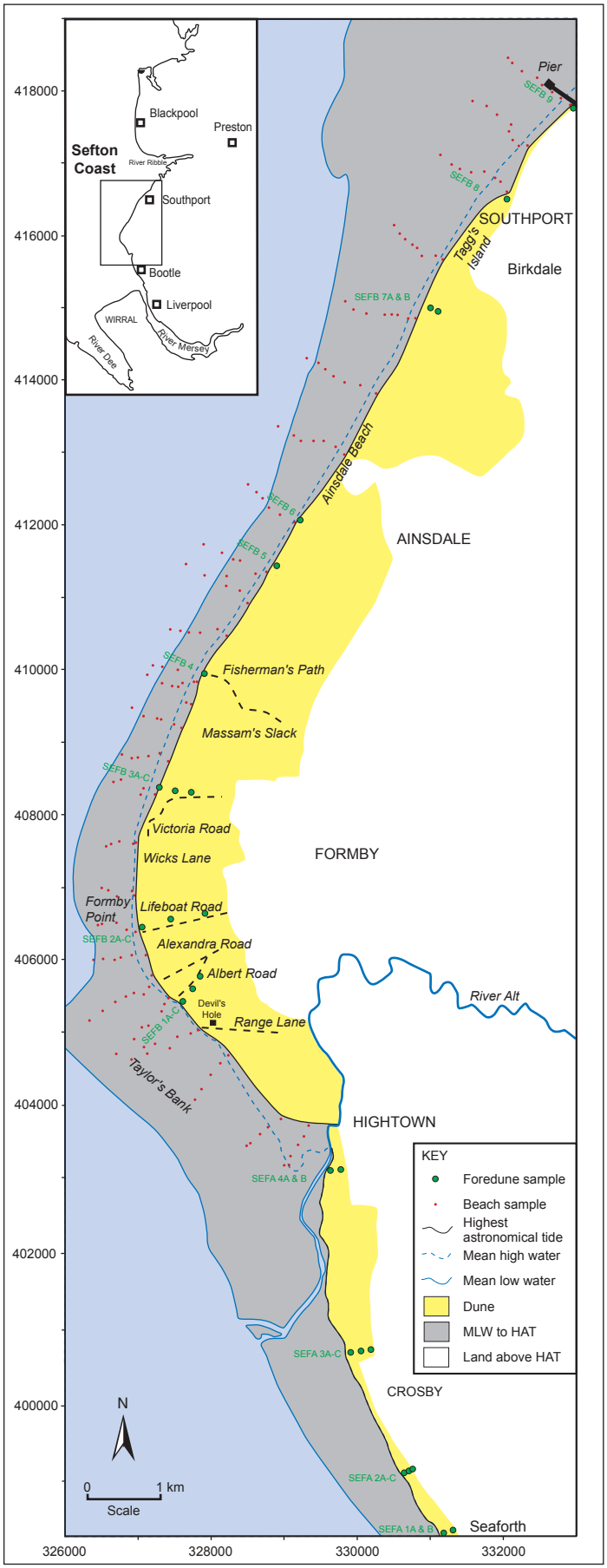

Figure 5.2 The main localities on the Sefton coast mentioned in this report, and location of dune samples collected in this study. Beach sample locations refer to results presented in Jay (1998).

Figure 5.3 Aerial photograph of the Sefton coast taken *c*. 2000. Active large-scale sand blowing is restricted mainly to locations around Formby Point between Lifeboat Road and Fisherman's Path. Source: Google Earth.

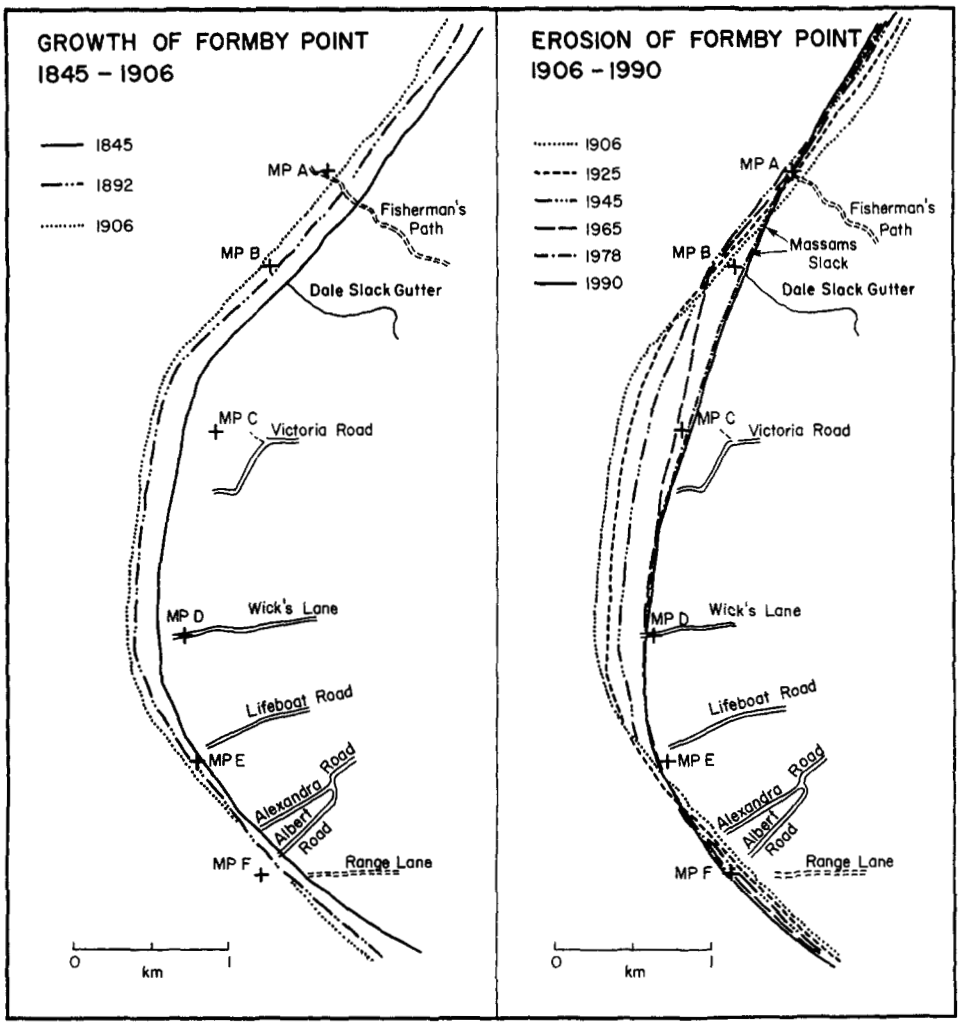

Figure 5.4 Growth of Formby Point 1845-1906 and erosion 1906-1990, based on Ordnance Survey maps and aerial photographs. After Pye (1991).

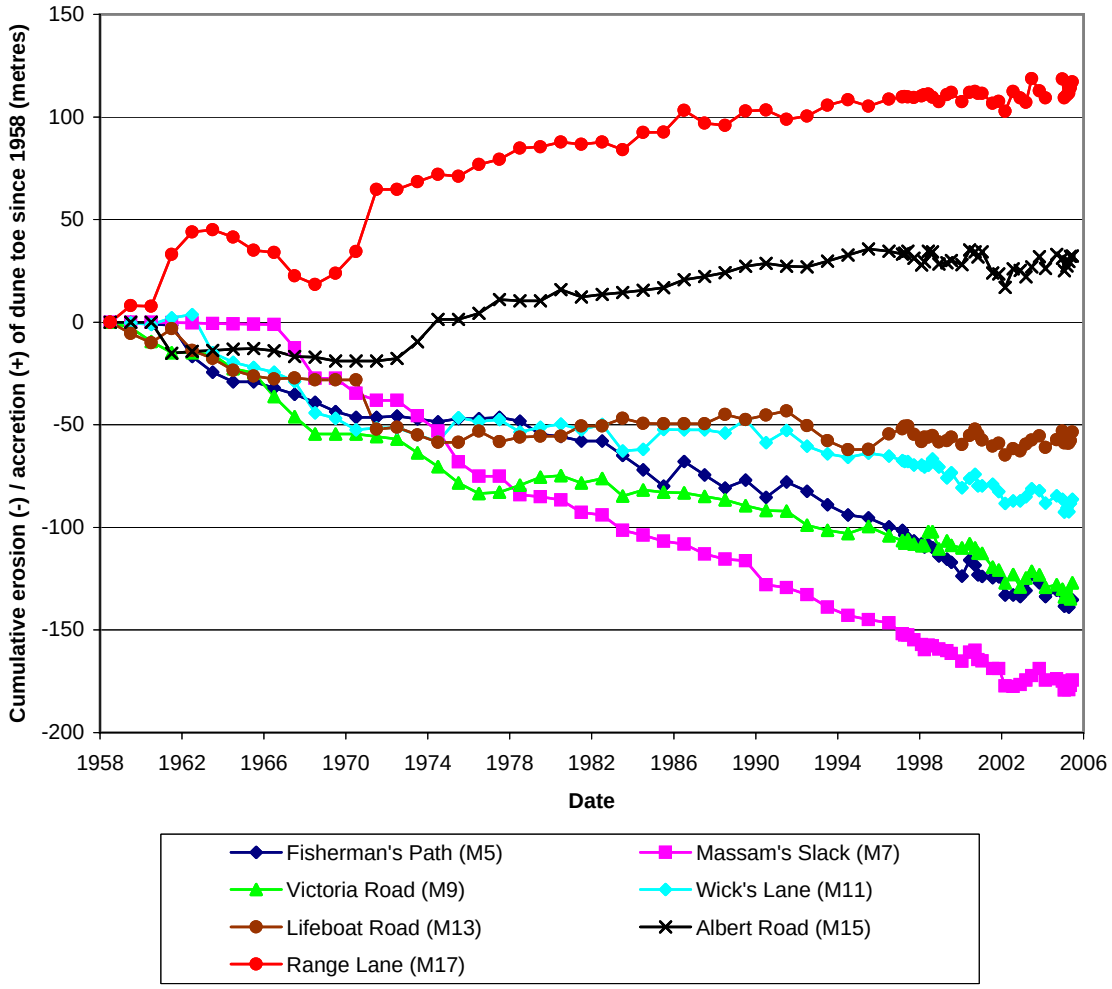

Figure 5.5 Frontal dune erosion and accretion measured at 7 different locations along the Sefton coast between 1958 and 2005. Data source: Surveys by Sefton Engineer and Surveyor's Department. Locations of monitoring stations are shown on Figure 5.2.

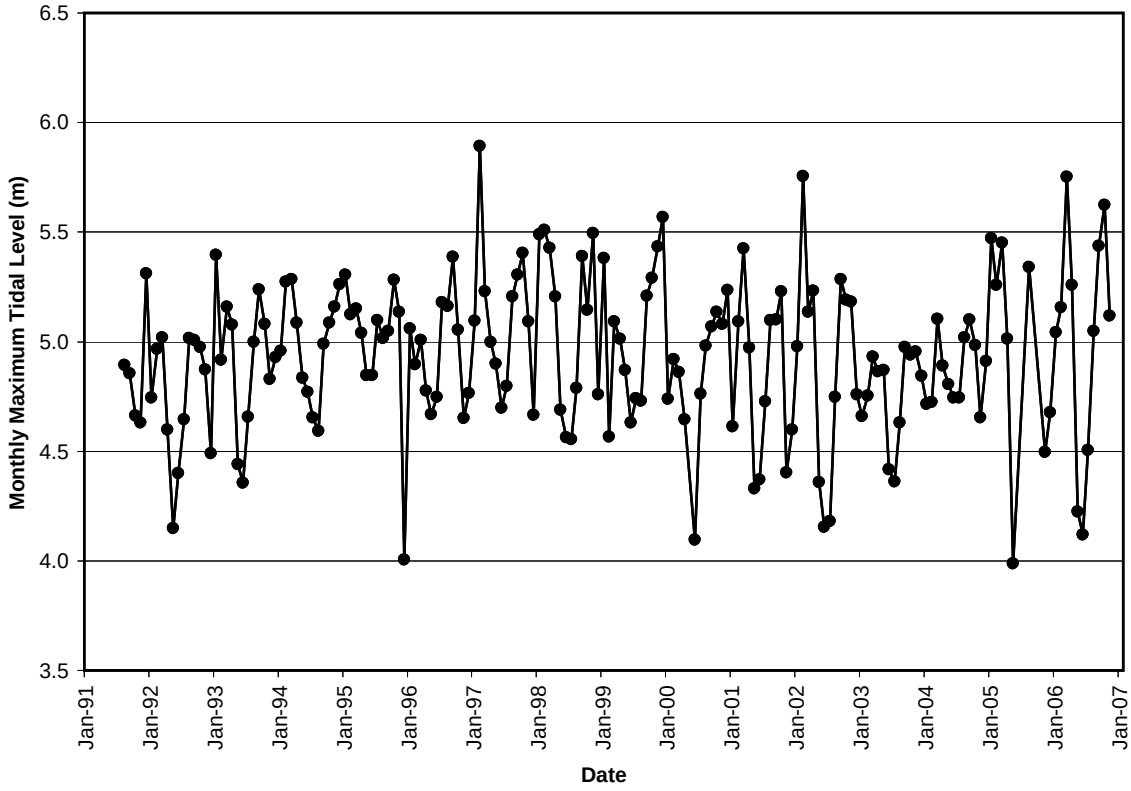

Figure 5.6 Monthly maximum tidal levels between 1990 and 2006 recorded at Liverpool. Data source: National Tide and Sea Level Facility.

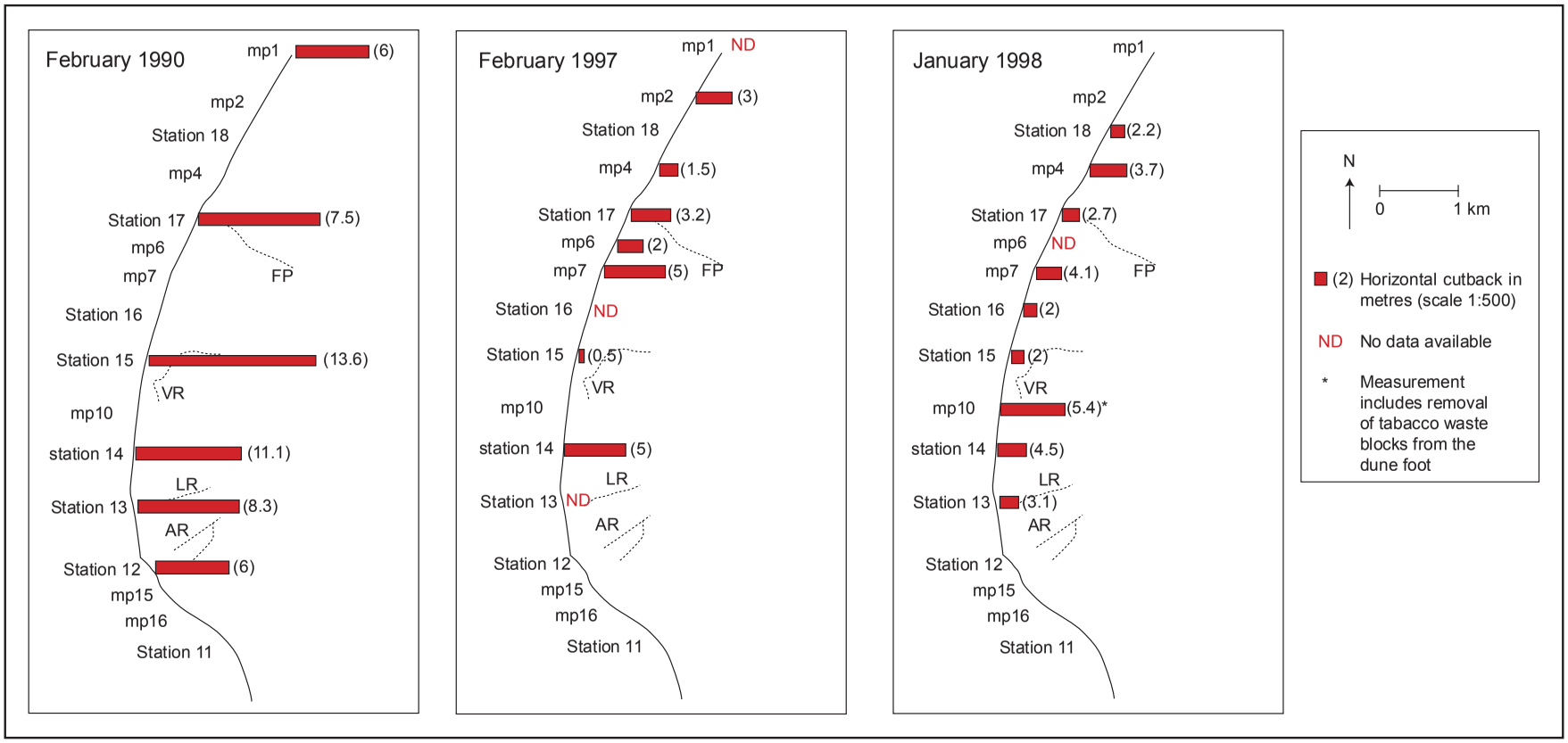

Figure 5.7 A comparison of the horizontal dune foot cutback on the Sefton coast resulting from the storms of February 1990, February 1997 and January 1998. FP is Fisherman's Path, VR is Victoria Road, LR is Lifeboat Road and AR is Alexandra Road. Data from Pye (1991) and Jay (1998).

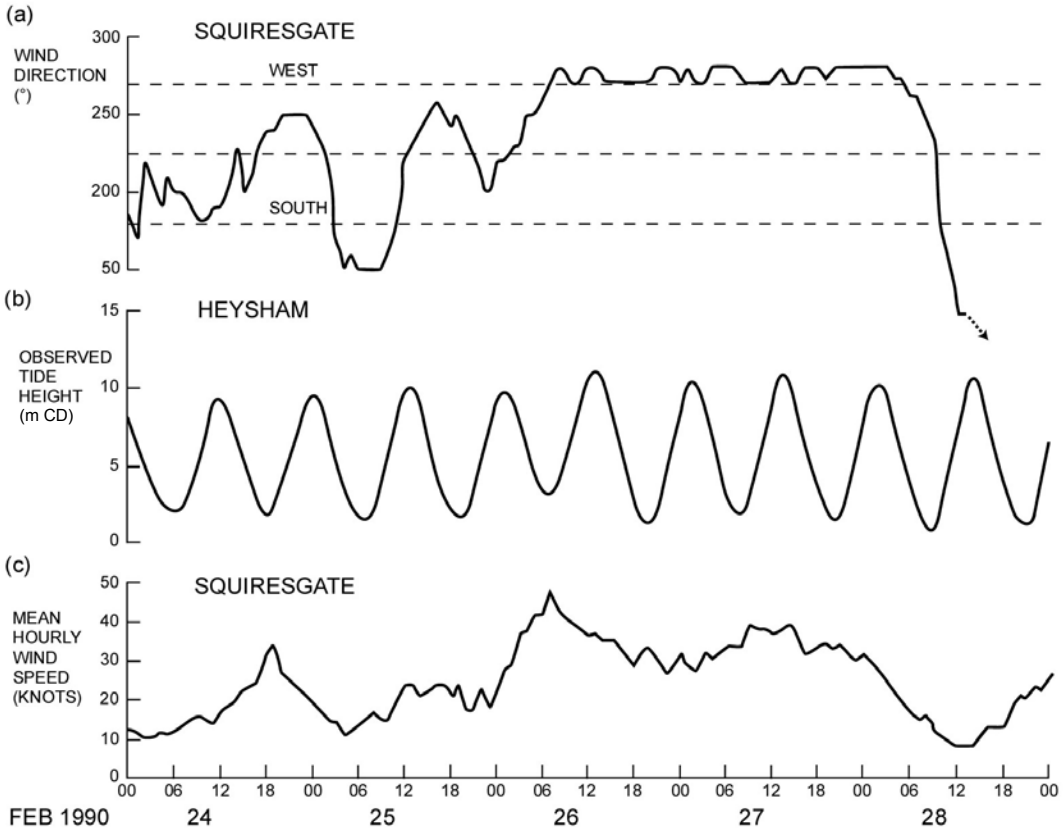

Figure 5.8 Meteorological data recorded at Squiresgate Airport, Blackpool, and tidal data recorded at Heysham during the period 24-28 February 1990: (a) wind direction; (b) tidal height; and (c) mean hourly wind speed. Severe frontal erosion at Formby Point occurred between 0000 hrs on 26 February and 0600 hrs on 28th February when five high tides coincided with strong winds from a westerly direction. Fortunately, the strongest winds around 0600 hrs on 26 February coincided with low water. The highest resultant tide, including a significant storm surge component, occurred around 1200 hrs on 26 February, causing the worst of the observed erosion. After Pye (1991).

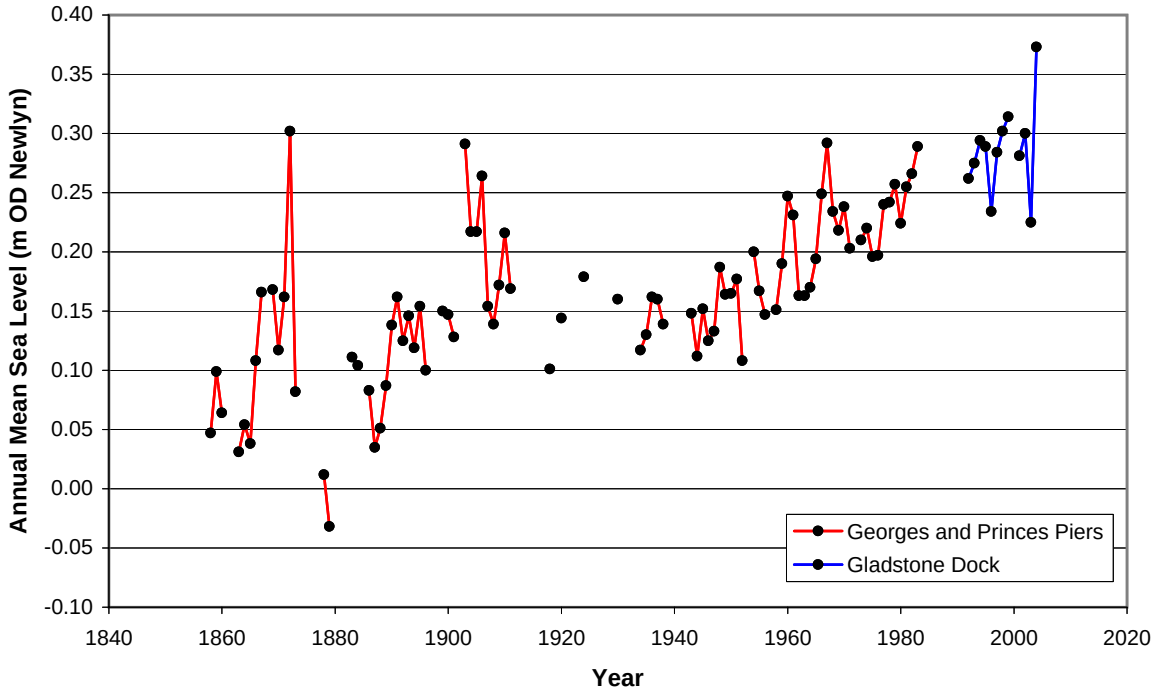

Figure 5.9 Annual mean sea level recorded at Liverpool (George and Princes Piers and Gladstone Dock). Data source: Permanent Service for Mean Sea Level.

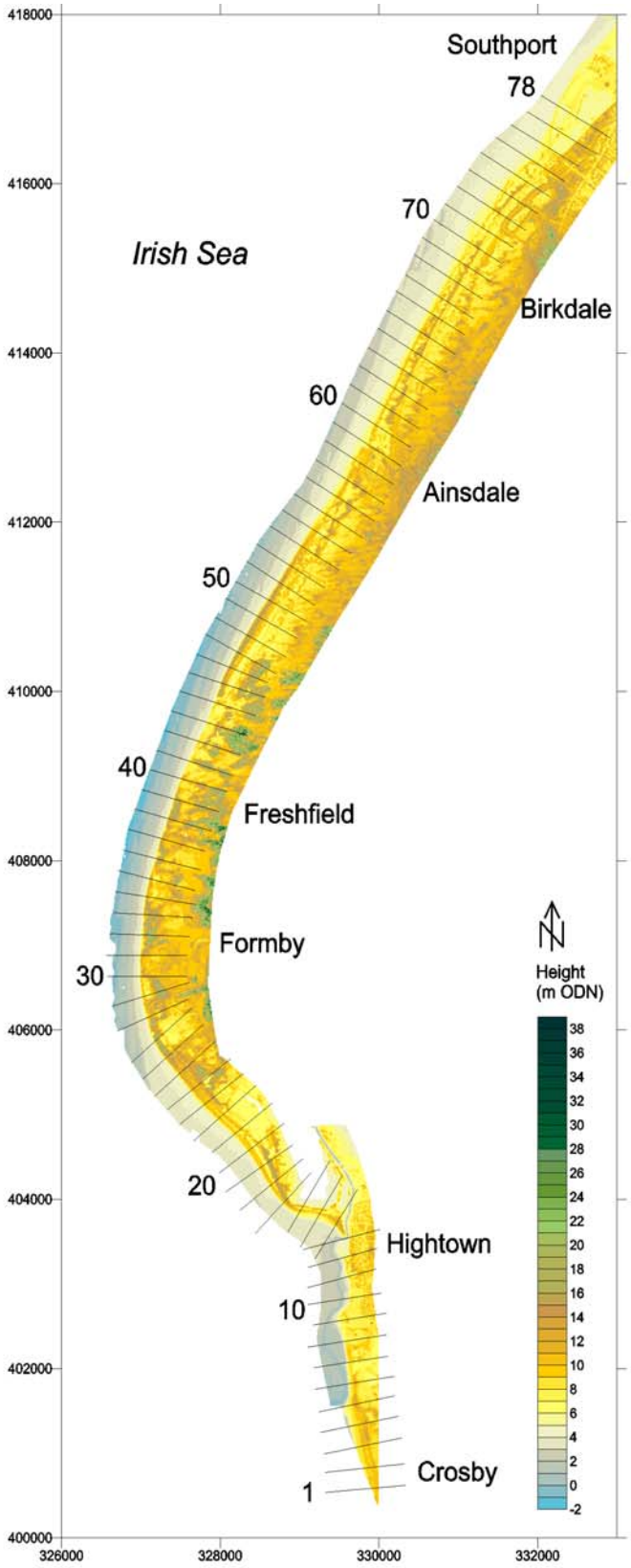

Figure 5.10 Digital terrain model of the Sefton coast, derived from lidar data flown in March 1999.

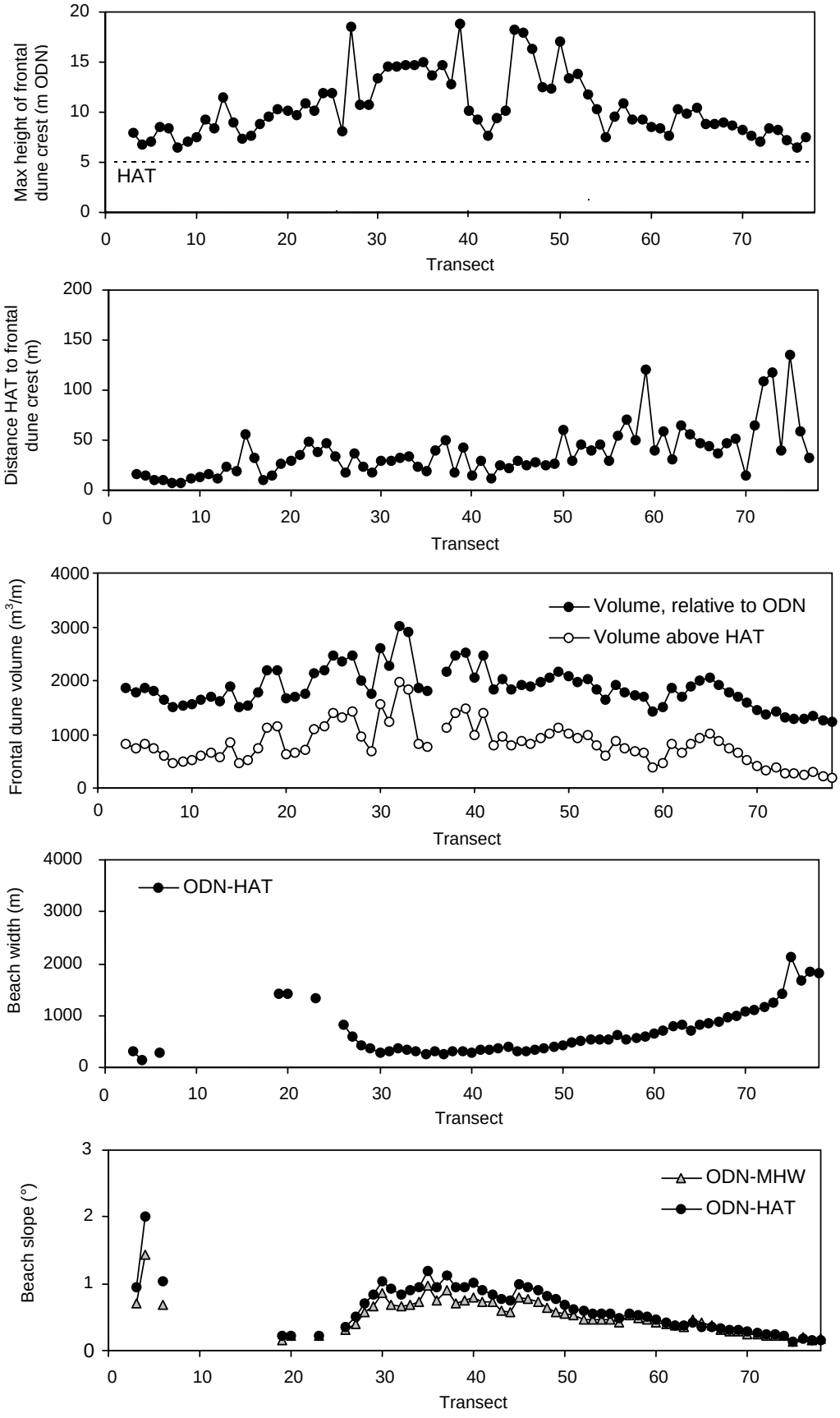

Figure 5.11 Longshore variation in beach and dune morphometric parameters derived from lidar data, Sefton coast. Transect positions are shown on Figure 5.10.

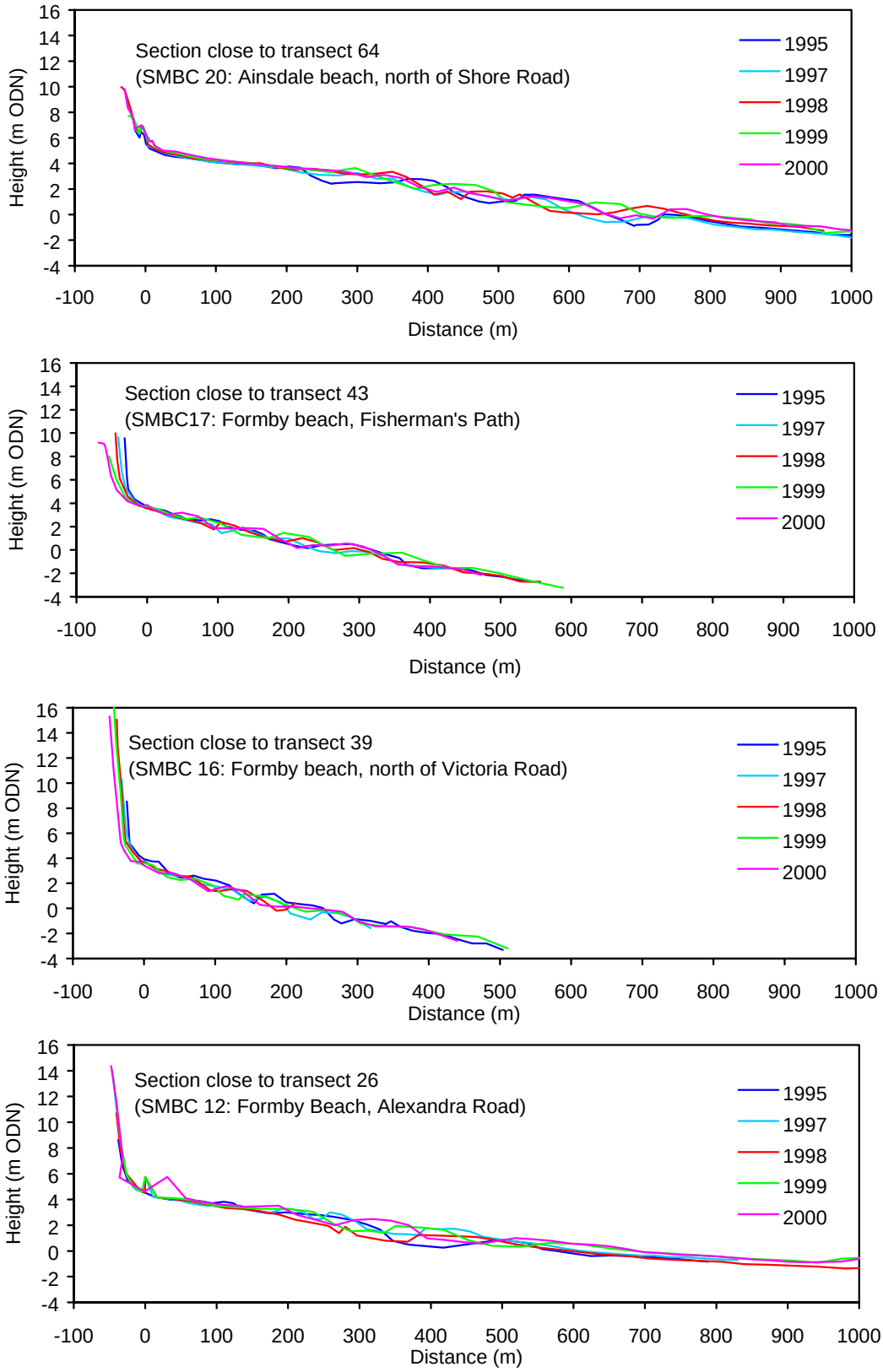

Figure 5.12 Changes in beach profiles on the Sefton Coast between 1995 and 2000, based on surveys by Sefton Metropolitan Borough Council.

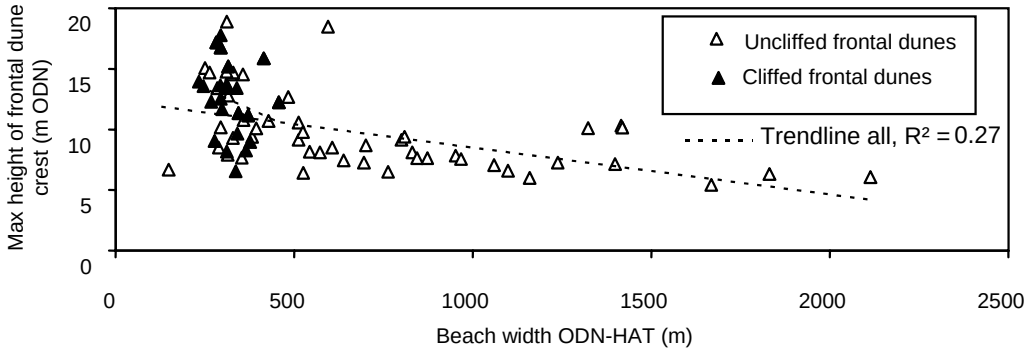

Figure 5.13 Width of beach between ODN and HAT versus maximum height of the frontal dune crest, Sefton coast, derived from lidar data.

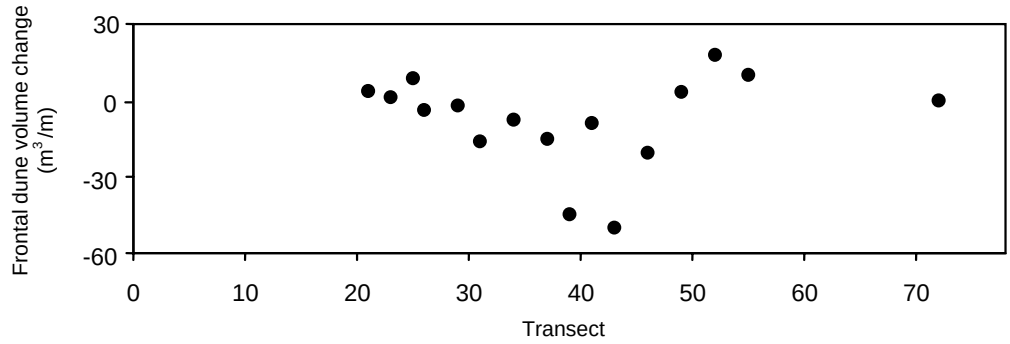

Figure 5.14 Changes in frontal dune volume measured by field survey between October 1996 and August 1998. +ve values indicate volume gain, and -ve values indicate volume loss. Data from Jay (1998).

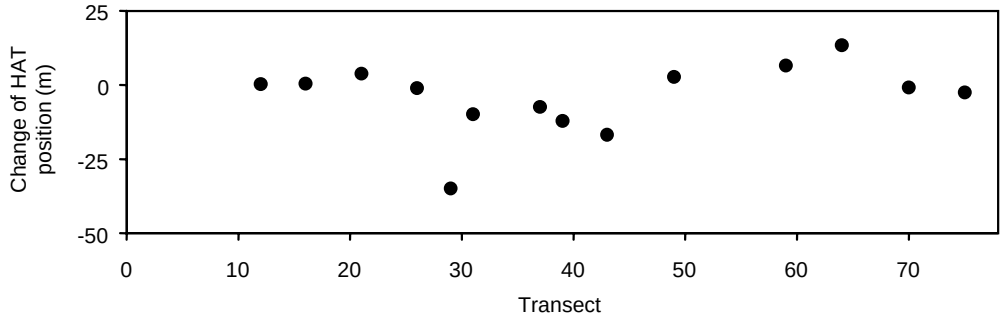

Figure 5.15 Changes in the position of HAT between August 1995 and 2000, based on ground survey data obtained from Sefton MBC. +ve values indicate advance, and -ve values indicate retreat.

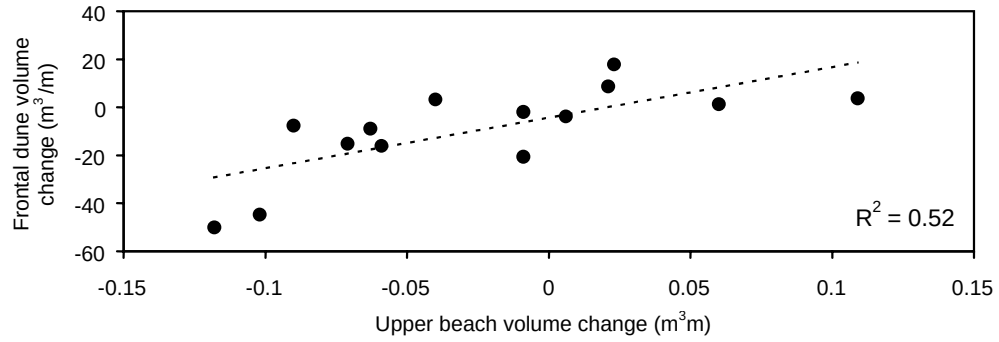

Figure 5.16 Relationship between changes in upper beach volume, measured between August 1995 and 1996, and changes in frontal dune volume, measured between October 1996 and August 1998. +ve values indicate volume gain, and -ve values indicate volume loss. Data from Jay (1998).

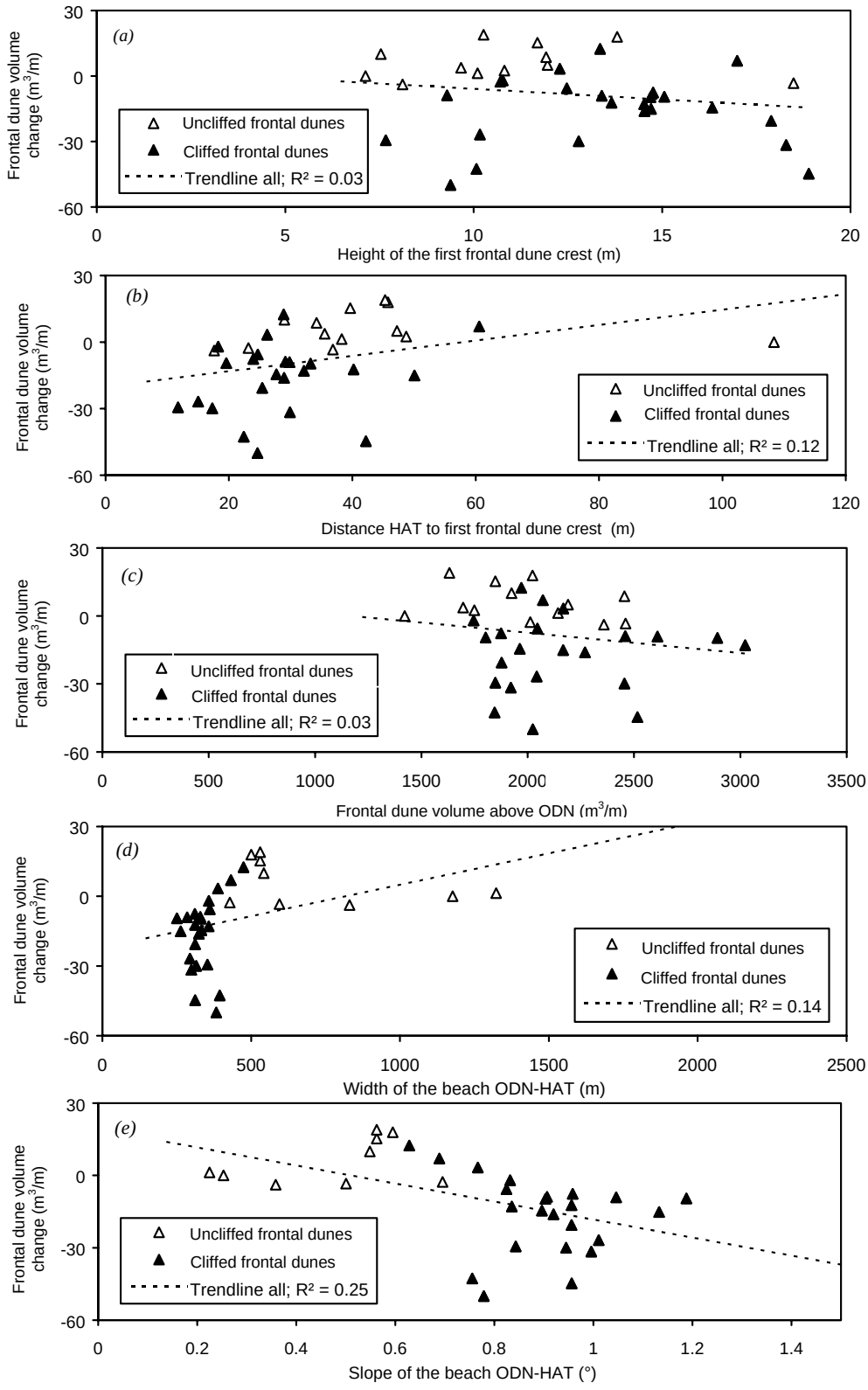

Figure 5.17 Change in frontal dune sediment volume between 1996 and 1998, reported by Jay (1998), related to morphometric parameters derived from lidar data flown in March 1999. Positive values indicate volume gain, and negative values indicate volume loss.

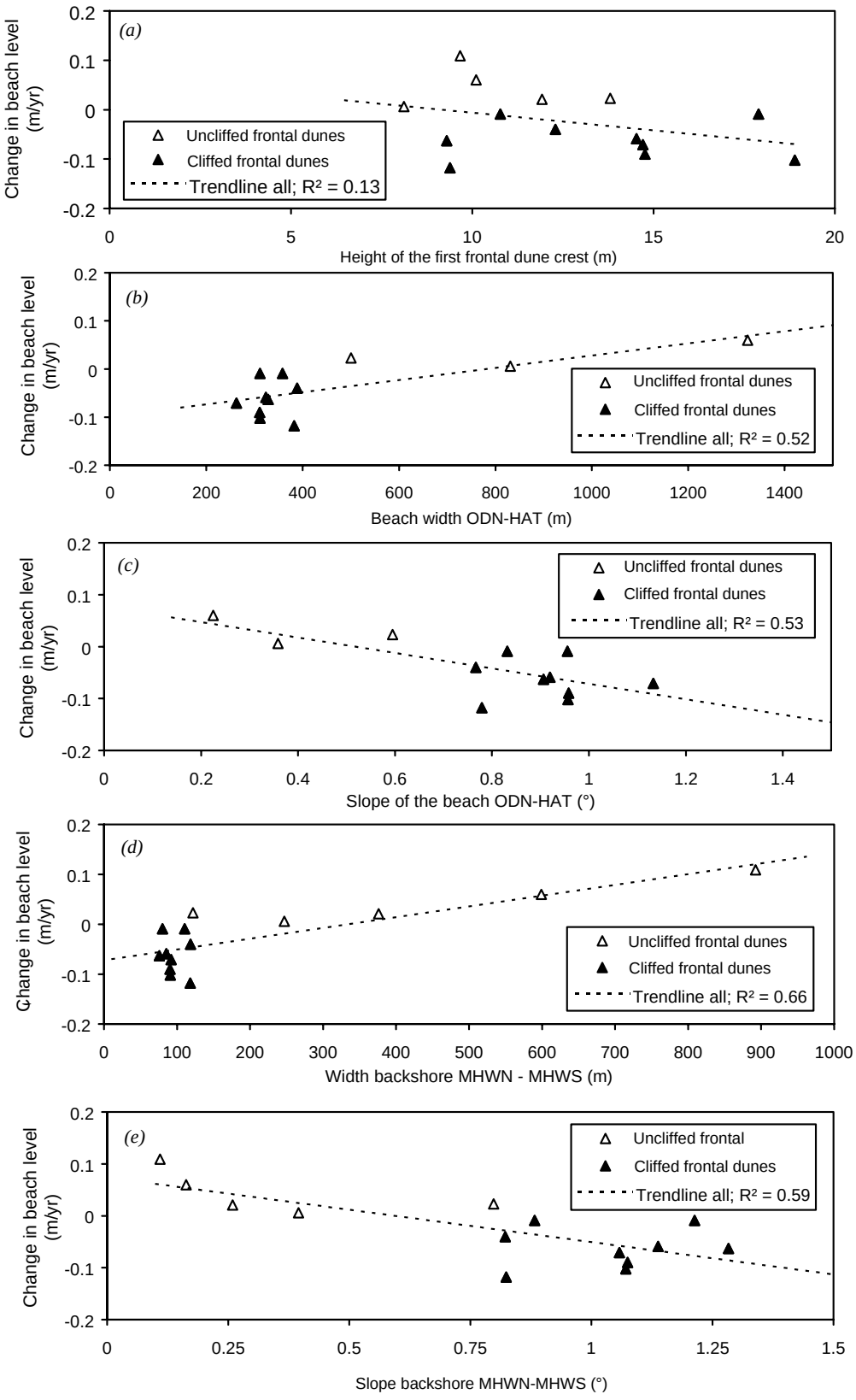

Figure 5.18 Changes in beach levels between 1991 and 1996, derived from surveys by Sefton MBC, related to morphometric parameters derived from lidar data flown in March 1999. Positive values indicate the beach level has raised, whilst negative values indicate the beach level has lowered.

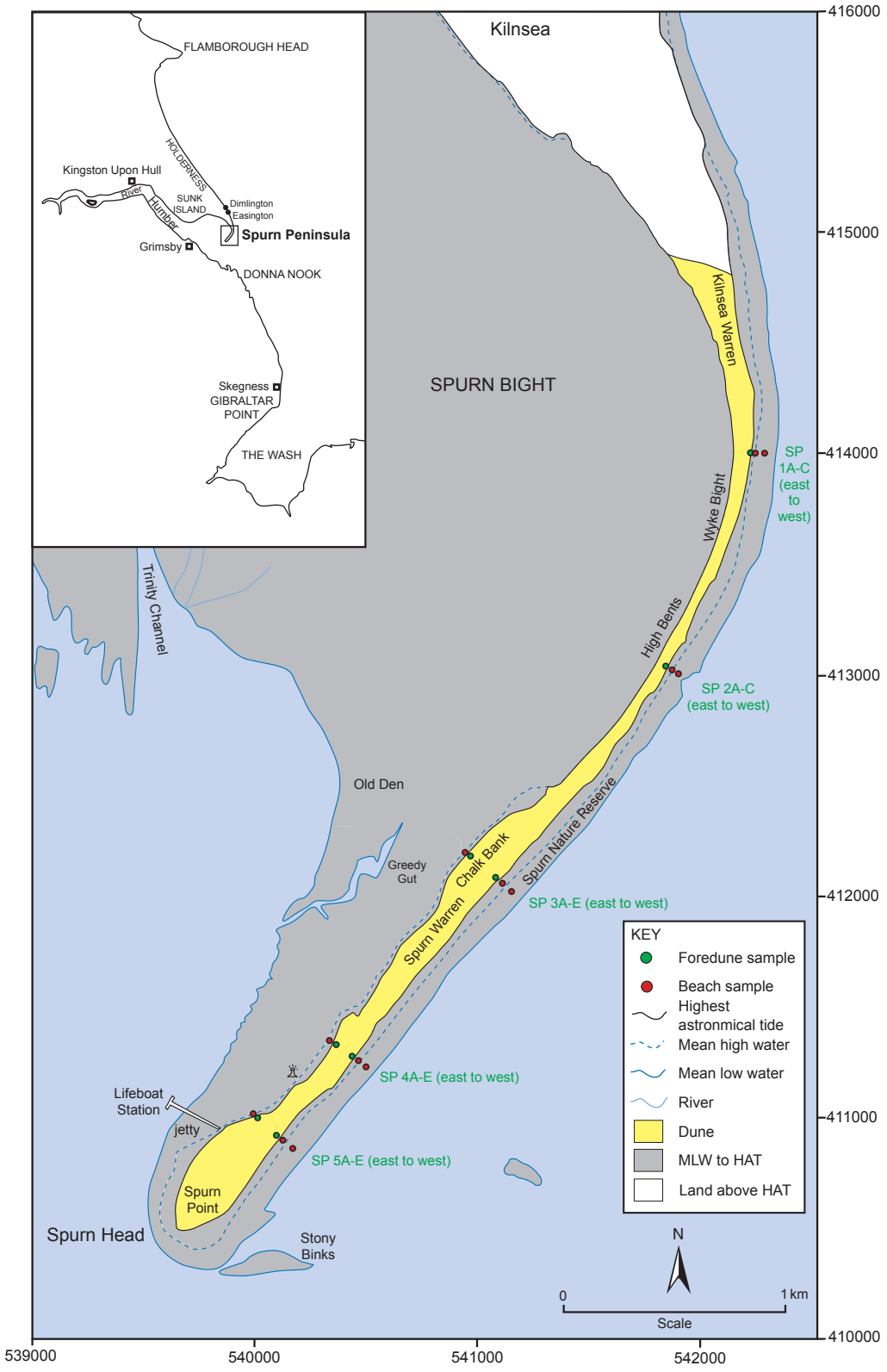

Figure 5.19 Map of Spurn Peninsula showing dune and beach sediment sampling locations. Further information about the beach sediments is contained in Saye (2003).

Figure 5.20 Oblique aerial photograph of Spurn Head, taken in 1996. Note the marked wave refraction around the end of the spit and northerly transport of sand up the landward side. Source: tlfe.org.uk.

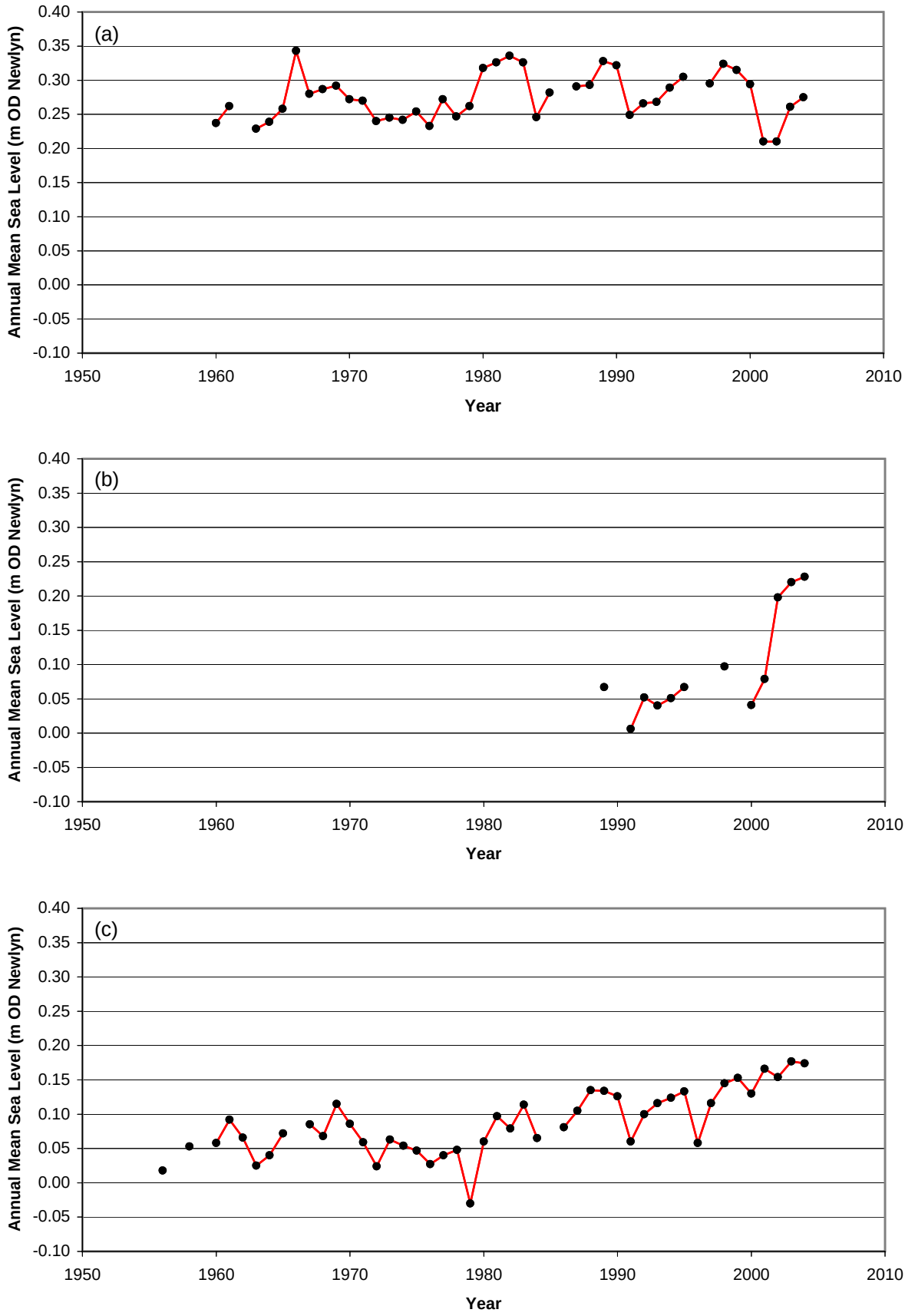

Figure 5.21 Annual mean sea level recorded at: (a) Immingham; (b) Cromer; and (c) Lowestoft. Data source: Permanent Service for Mean Sea Level.

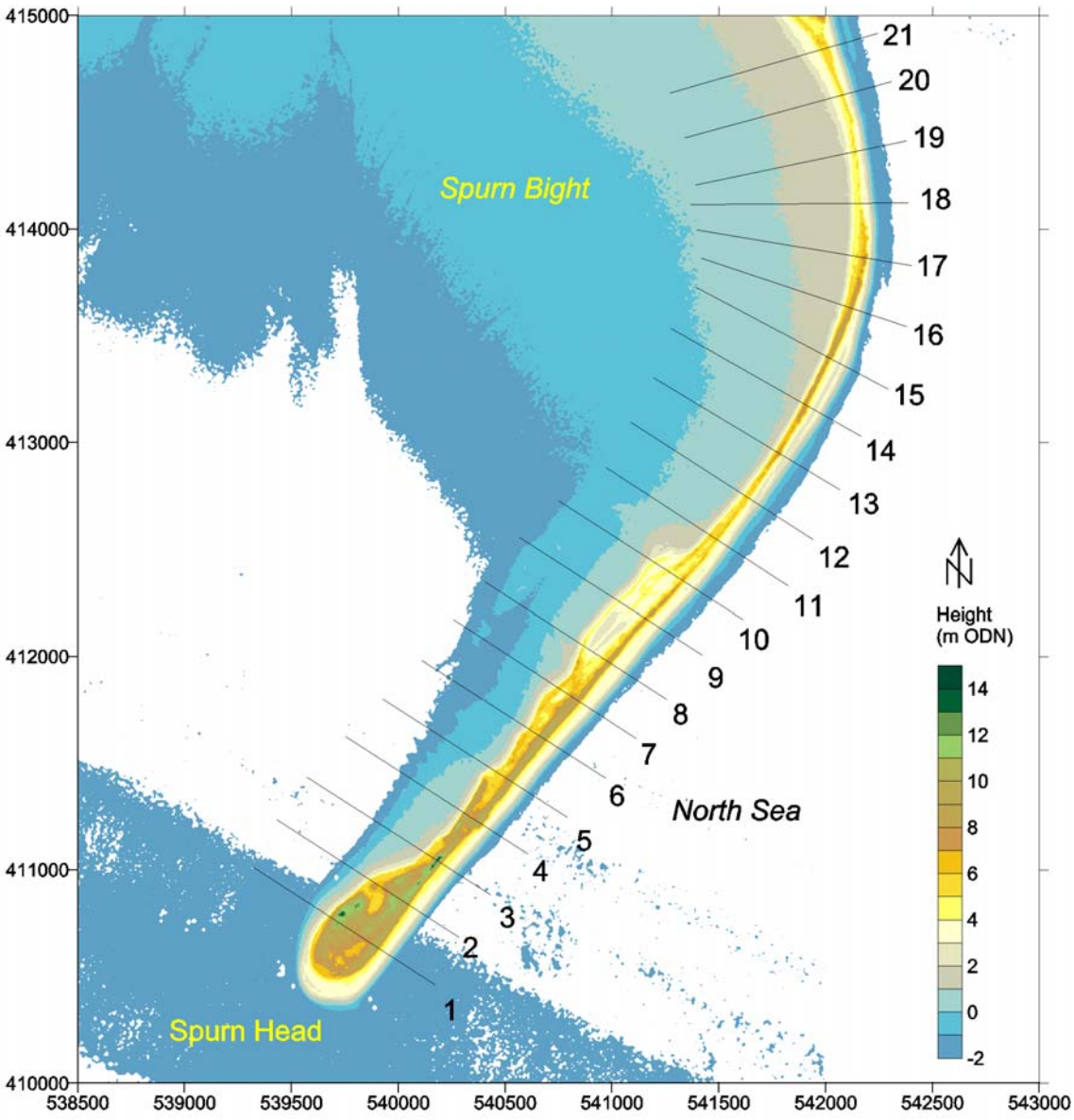

Figure 5.22 Digital terrain model of Spurn Peninsula derived from lidar data flown in May 1999.

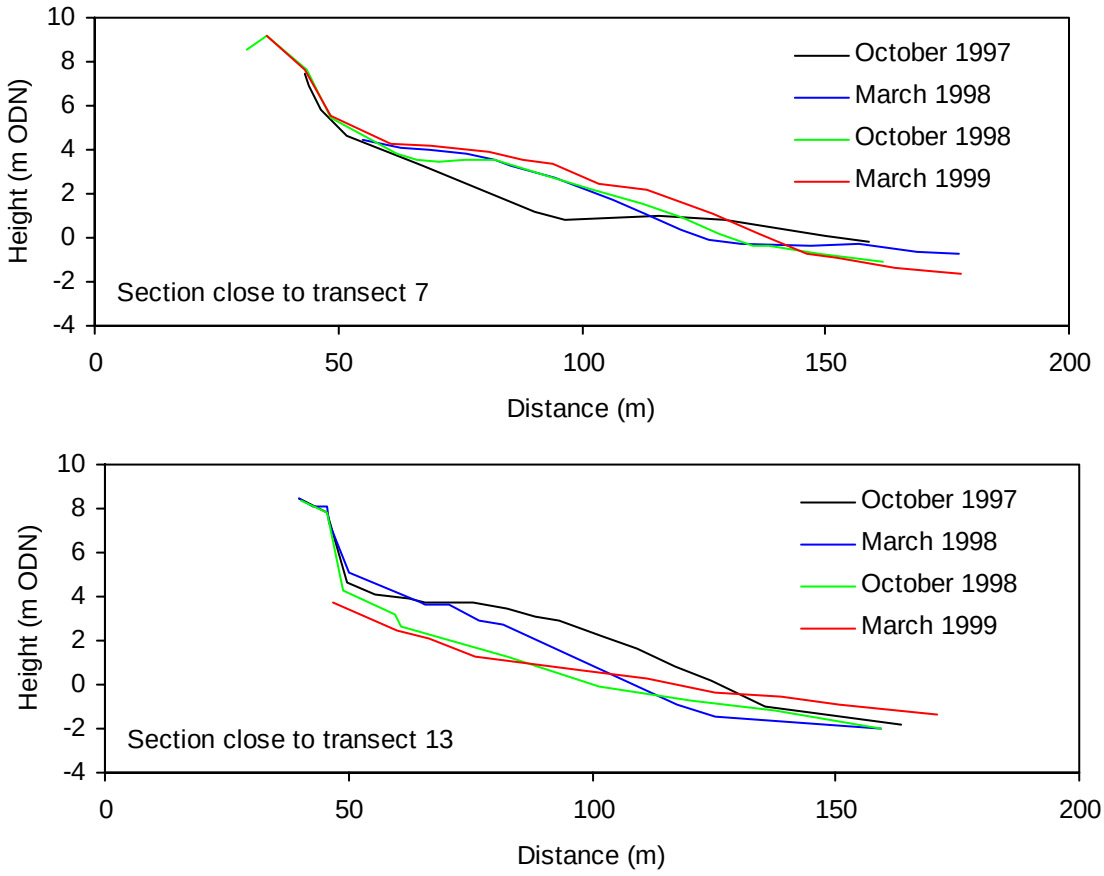

Figure 5.23 Surveyed beach cross-sections along the eastern side of Spurn Peninsula between 1997 and 1999. Data from East Riding of Yorkshire Council. Transect positions are shown in Figure 5.22.

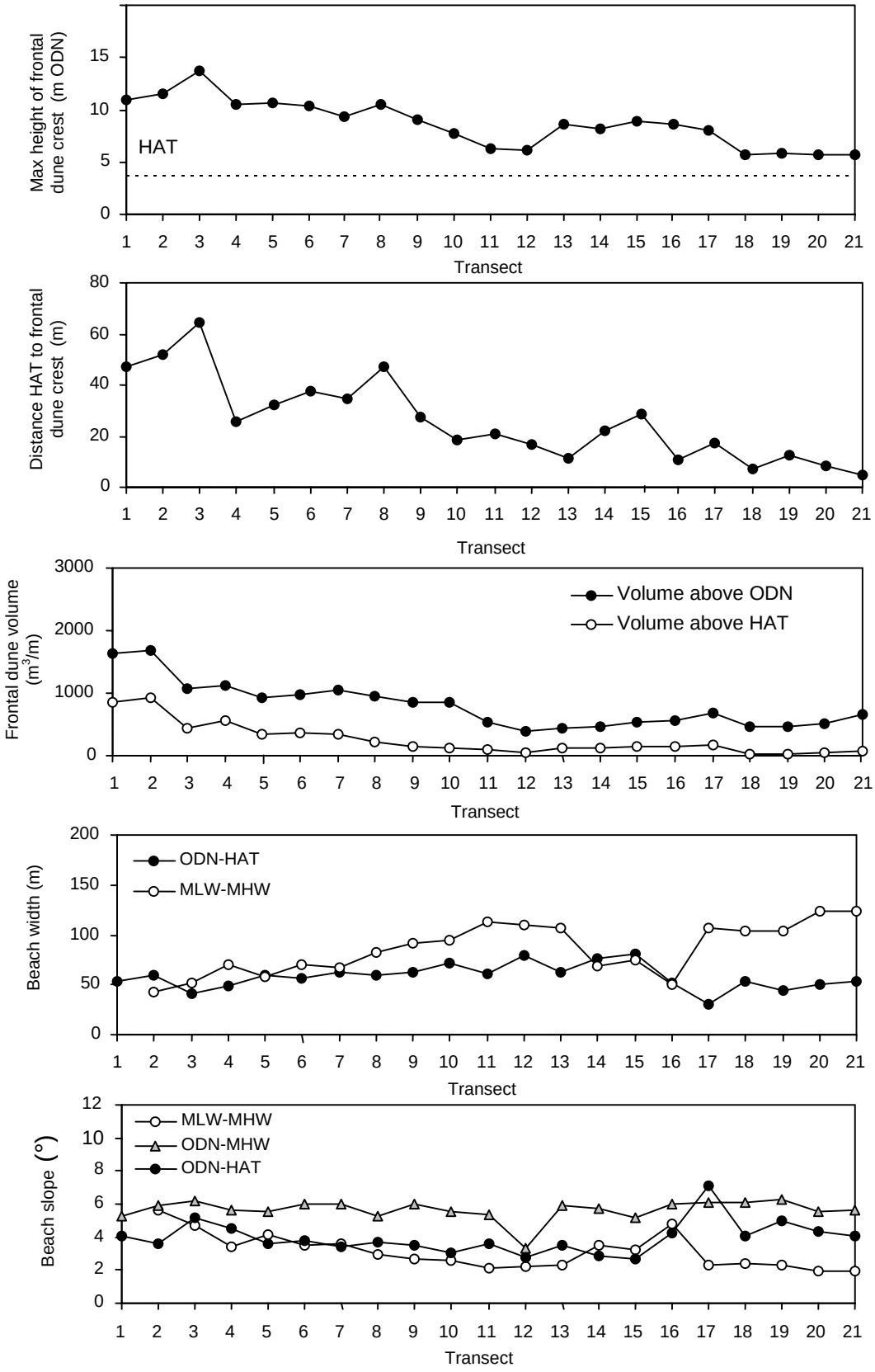

Figure 5.24 Longshore variation in beach and dune morphometric parameters along Spurn Peninsula, derived from lidar data flown in May 1999. Transect positions are shown in Figure 5.22.

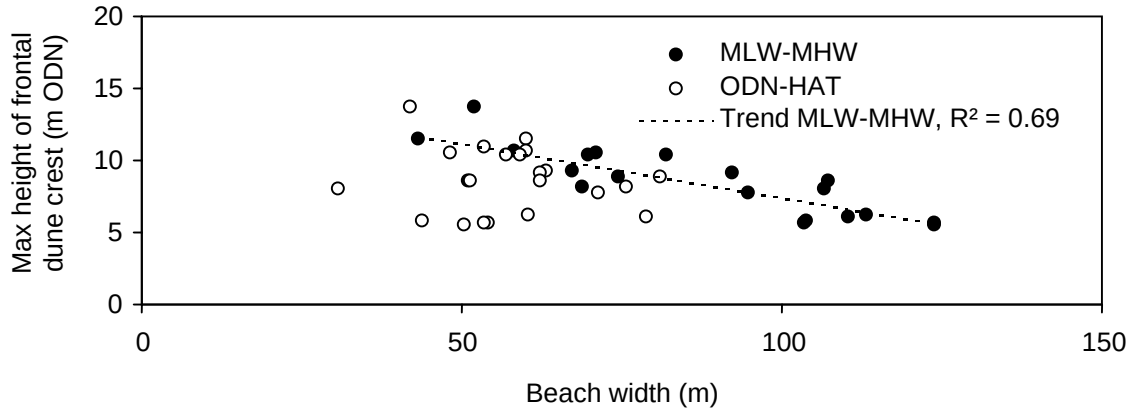

Figure 5.25 Relationship between beach width and maximum height of the frontal dune crest along Spurn Peninsula, derived from lidar data flown in May 1999.

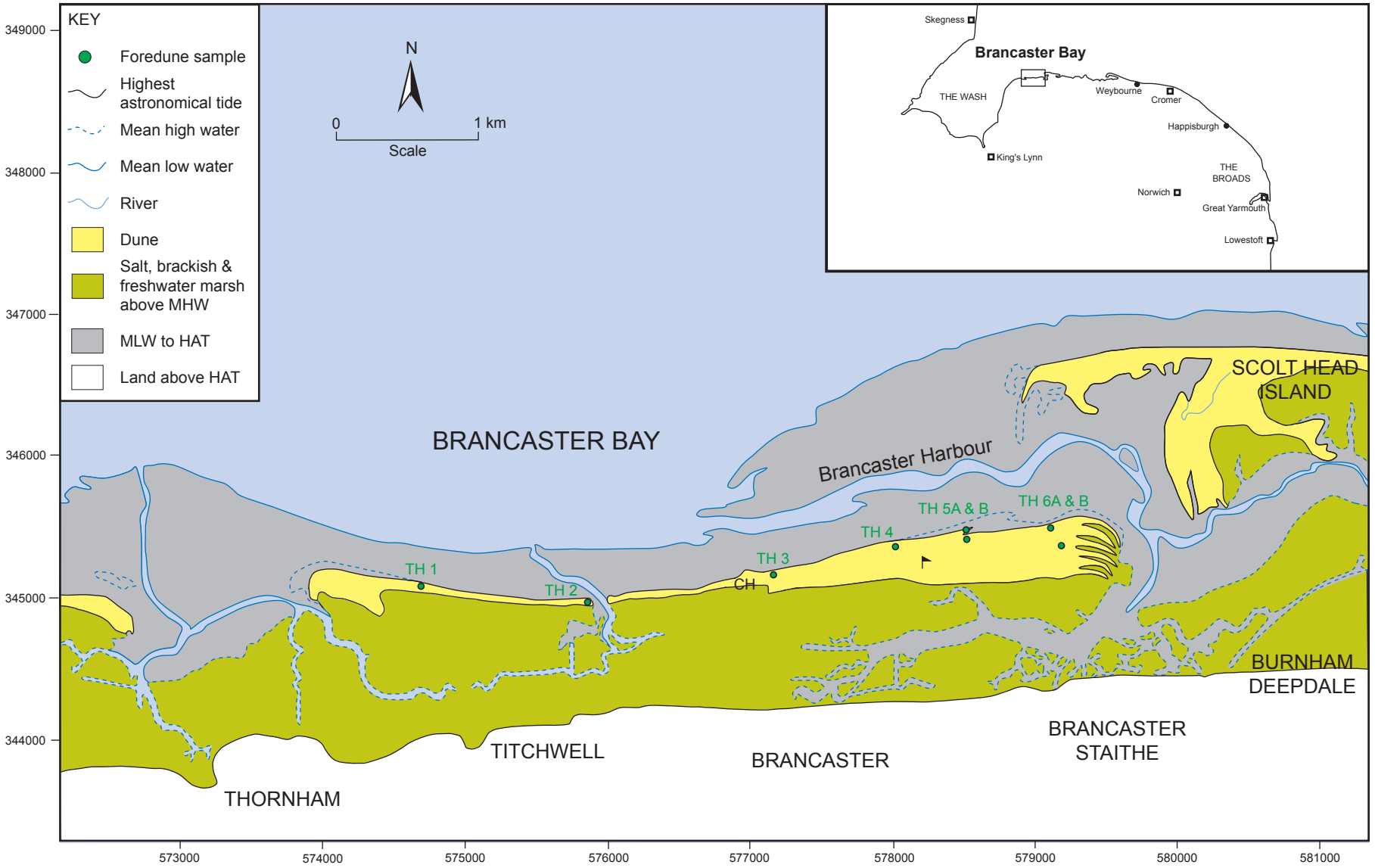

Figure 5.26 The main physical features of Brancaster Bay, showing dune sampling locations.

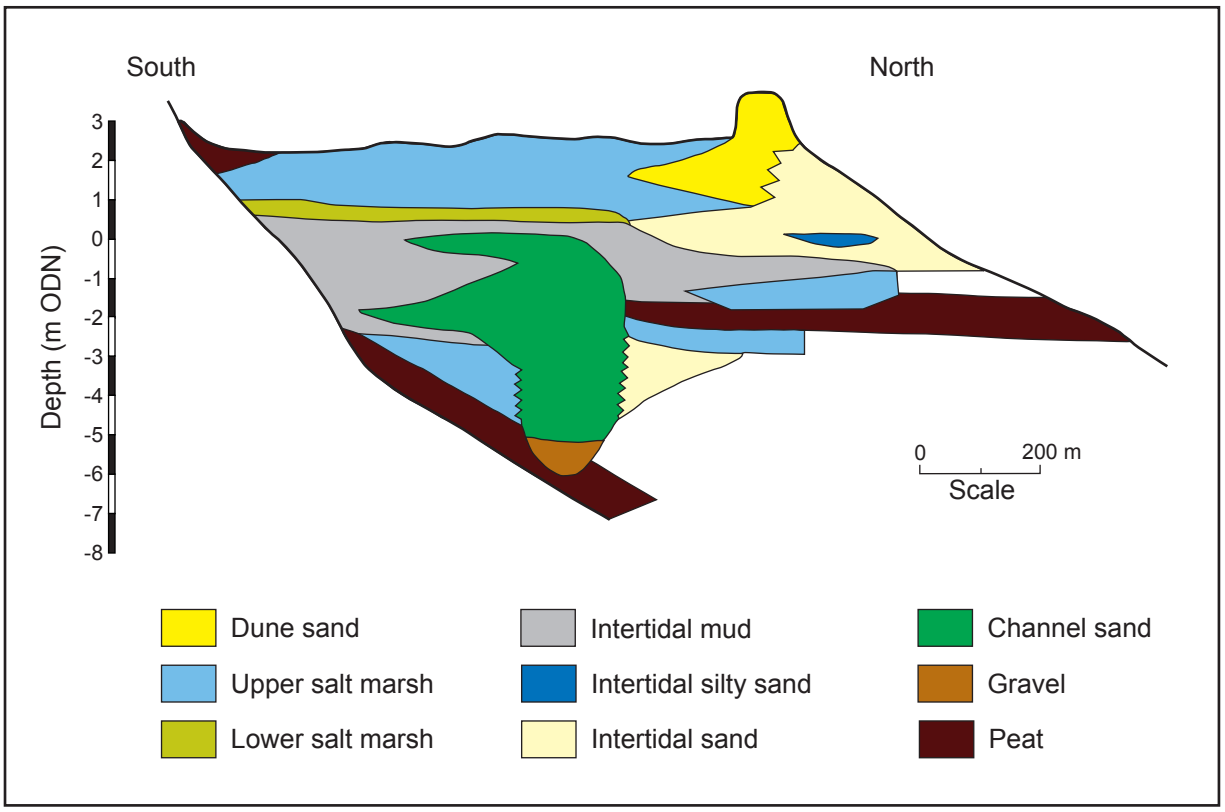

Figure 5.27 Cross-section showing the stratigraphy of Brancaster Bay, east of the golf clubhouse, based on drilling results (Funnell and Pearson, 1989).

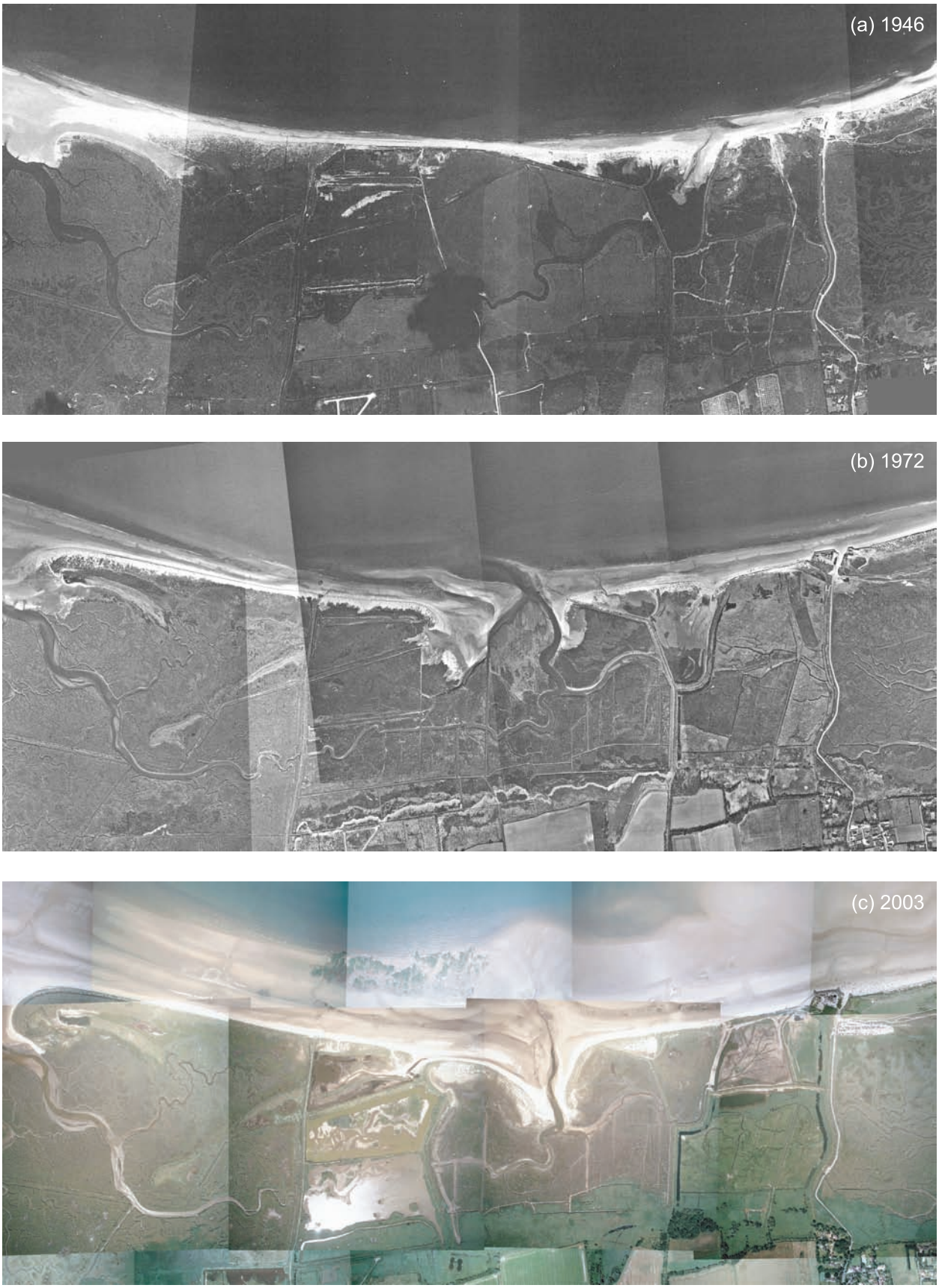

Figure 5.28 Historical aerial photographs of Brancaster Bay: (a) 1946 flown by the RAF; (b) 1972 flown by the Ordnance Survey; (c) 2003 flown by the Environment Agency. Photographs supplied by the National Monuments Record and the Environment Agency.

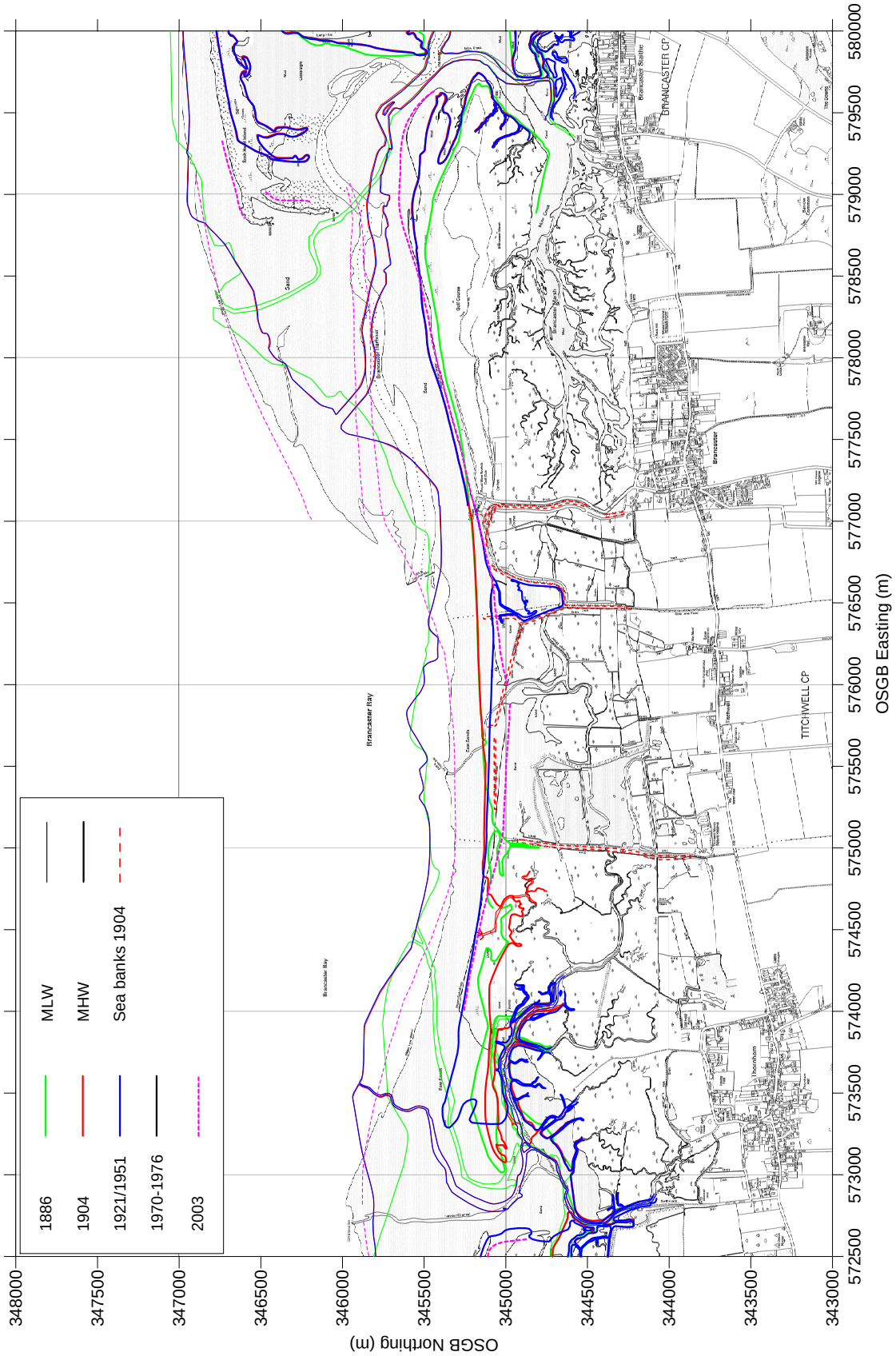

Figure 5.29 Historical positions of the coastline of Brancaster Bay digitised from Ordnance Survey maps surveyed in 1886, 1904, 1921 and 1970-1976, and aerial photography flown in 2003 by the Environment Agency.

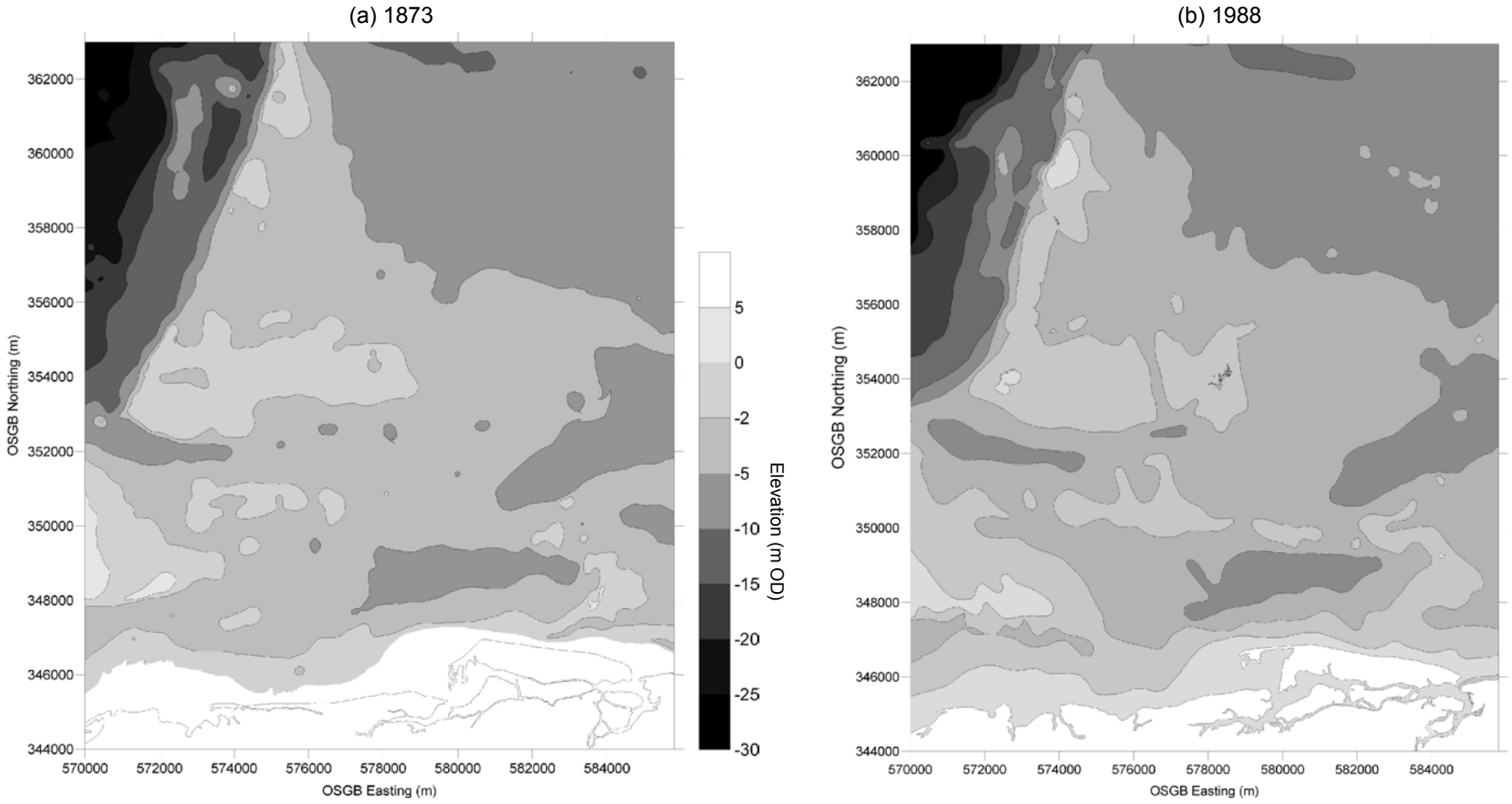

Figure 5.30 Bathymetric change in the offshore area adjacent to Brancaster Bay, digitised from Admiralty surveys published in 1873 and 1988.

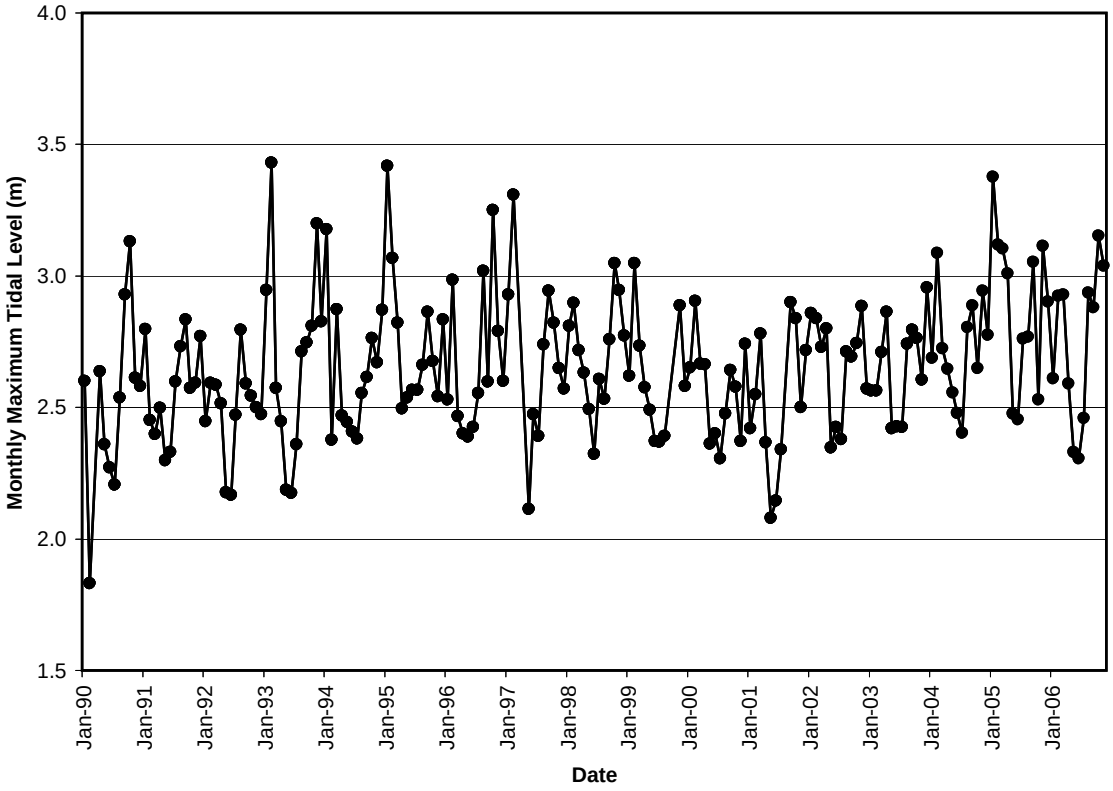

Figure 5.31 Monthly maximum tidal levels between 1990 and 2006 recorded at Cromer. Data source: National Tide and Sea Level Facility.

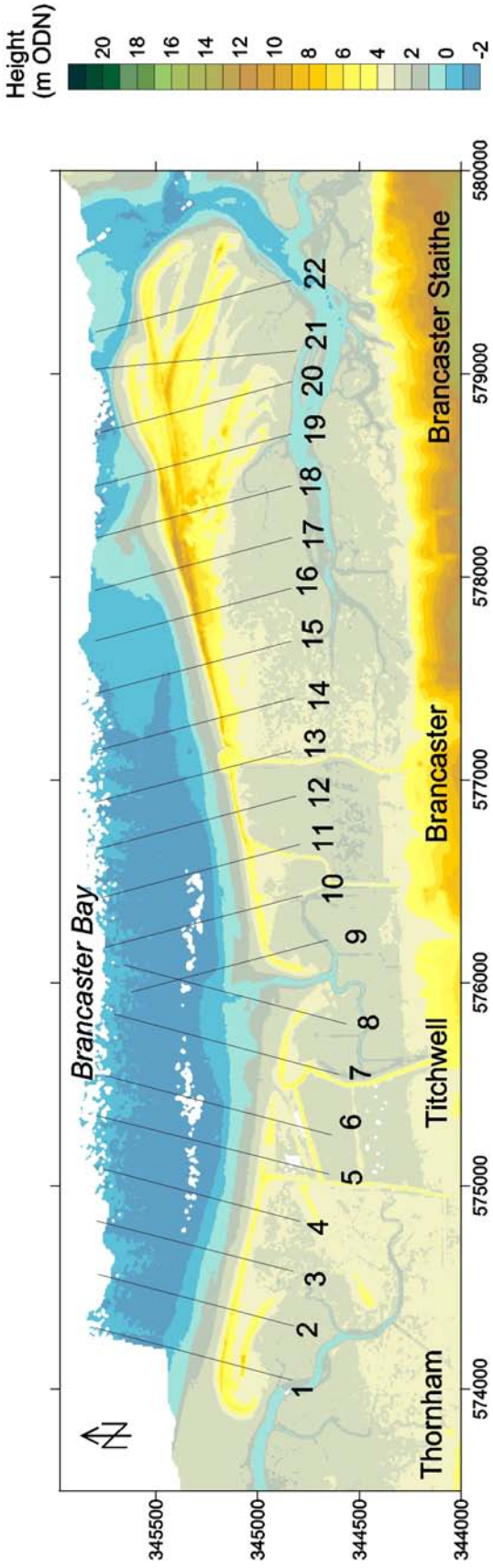

Figure 5.32 Digital terrain model of Brancaster Bay obtained from lidar data flown in March 1999.

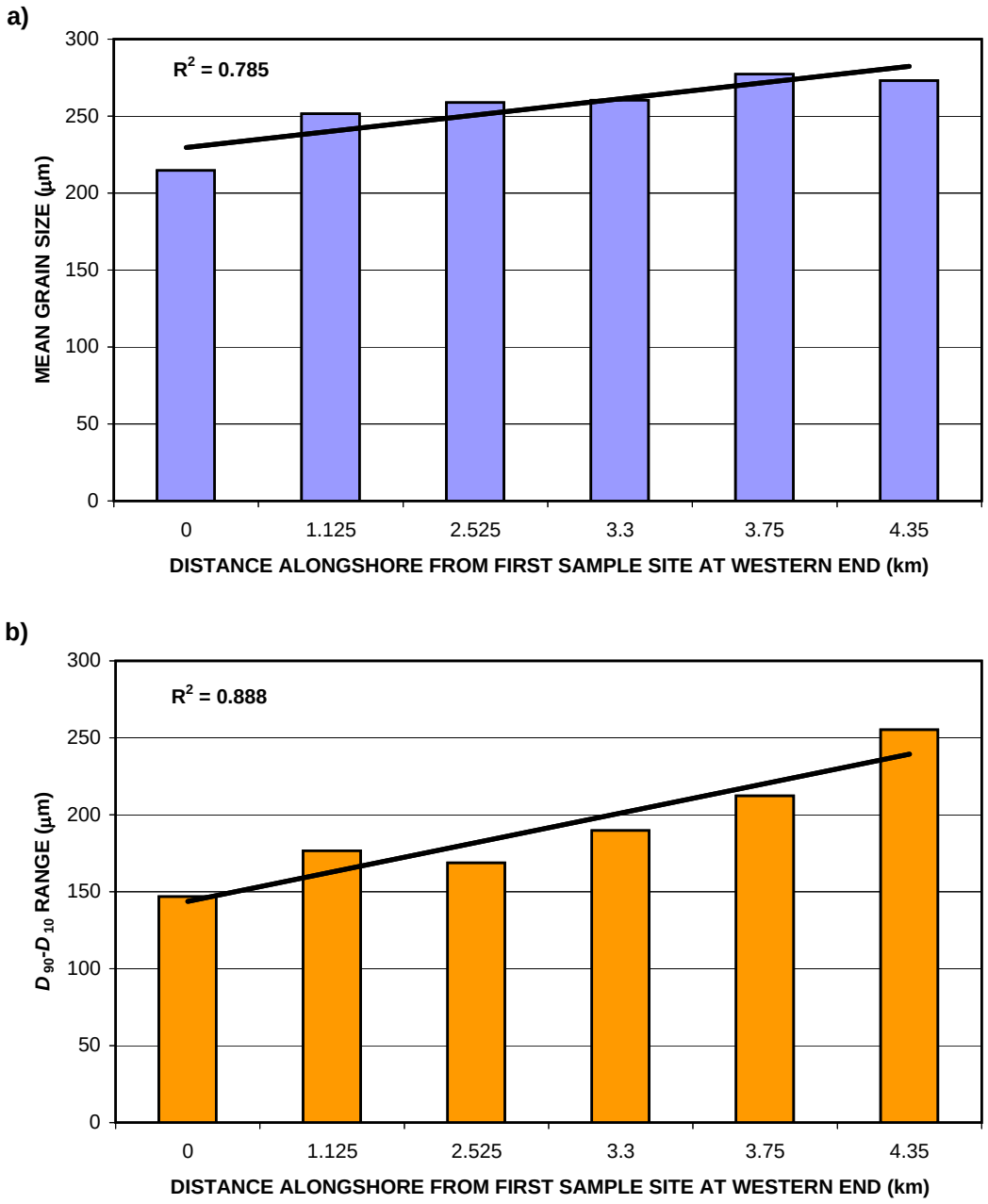

Figure 5.33 Variation in a) mean grain size and b) sorting (D_{90}-D_{10}) of frontal dune samples from west to east in Brancaster Bay. The sands become slightly coarser grained and more poorly sorted towards the east.

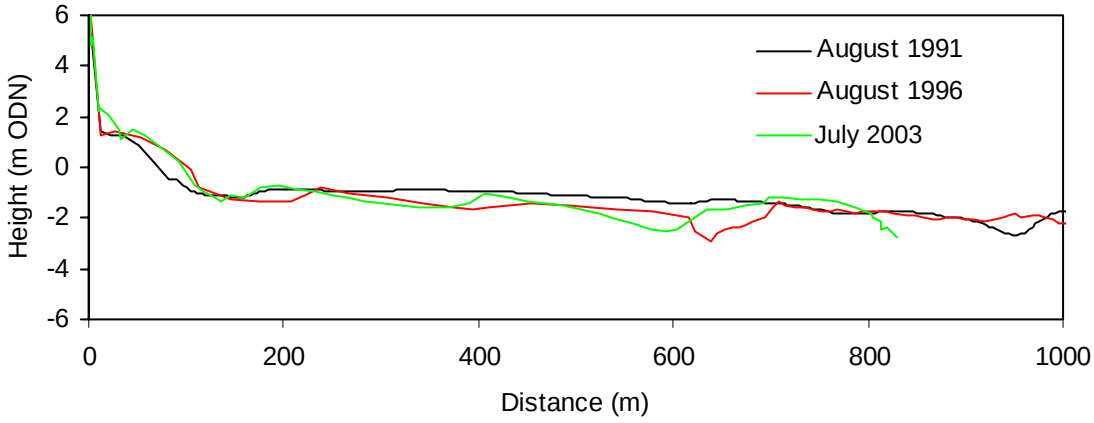

Figure 5.34 Topographic and bathymetric cross-sections on different dates near transect 13 (by the golf clubhouse). Data from the Environment Agency.

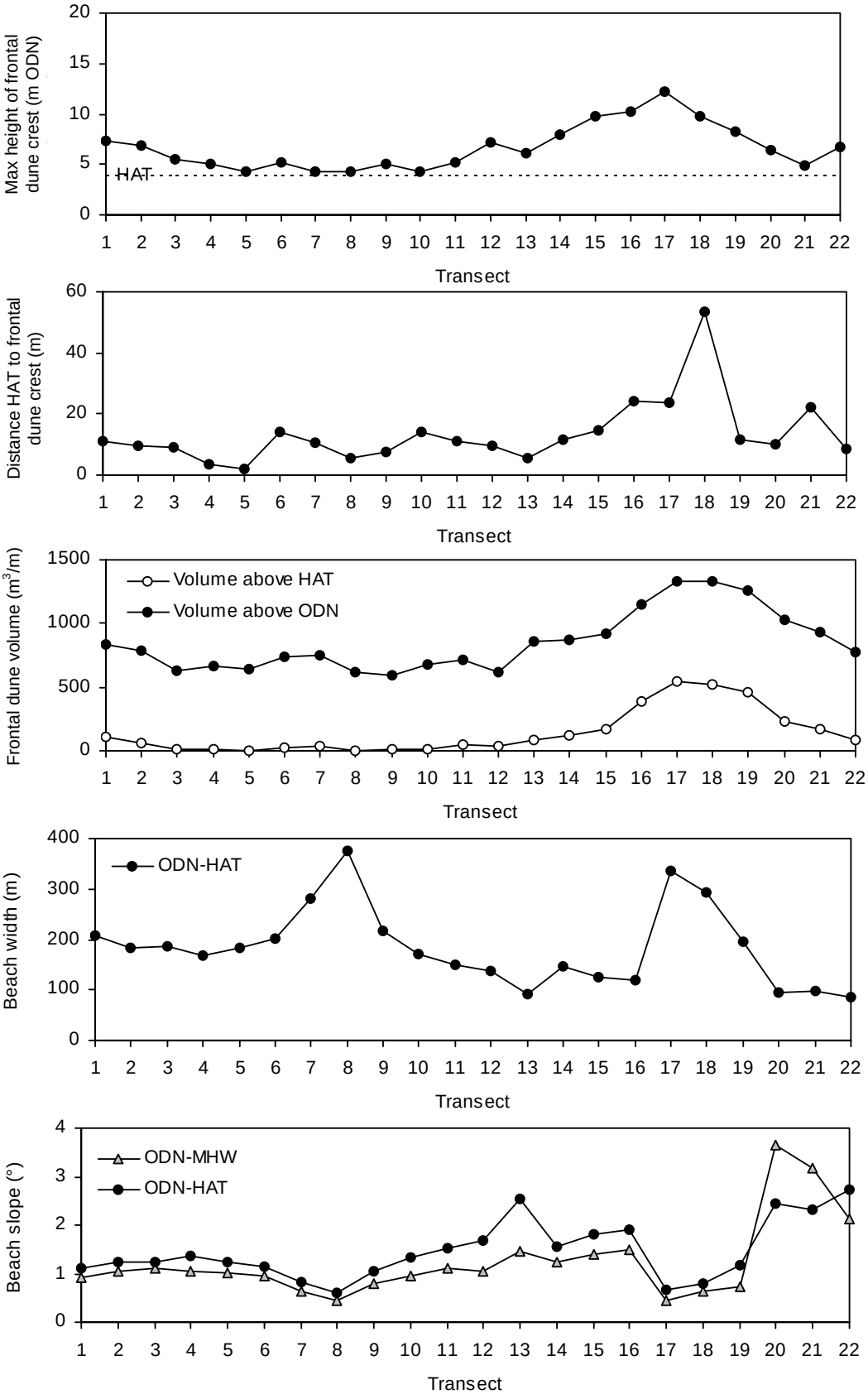

Figure 5.35 Longshore variation in beach and dune morphometric parameters derived from lidar data, Brancaster Bay. Transect positions are shown on Figure 5.32.

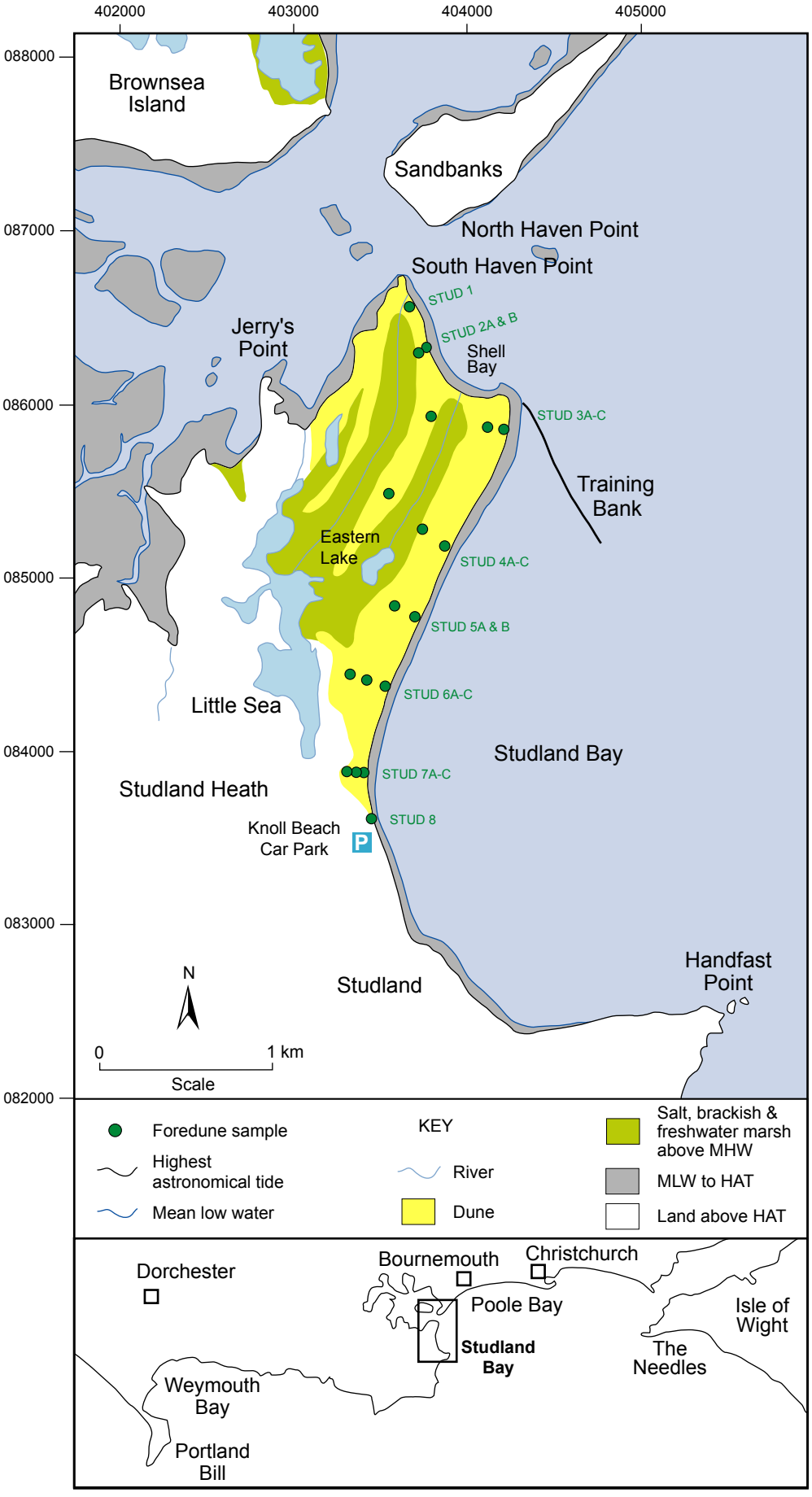

Figure 5.36 The main physical features of Studland Bay, showing dune sediment sampling locations.

Figure 5.37 Aerial photograph of Studland Bay, taken c. 2001. Source: Google Earth.

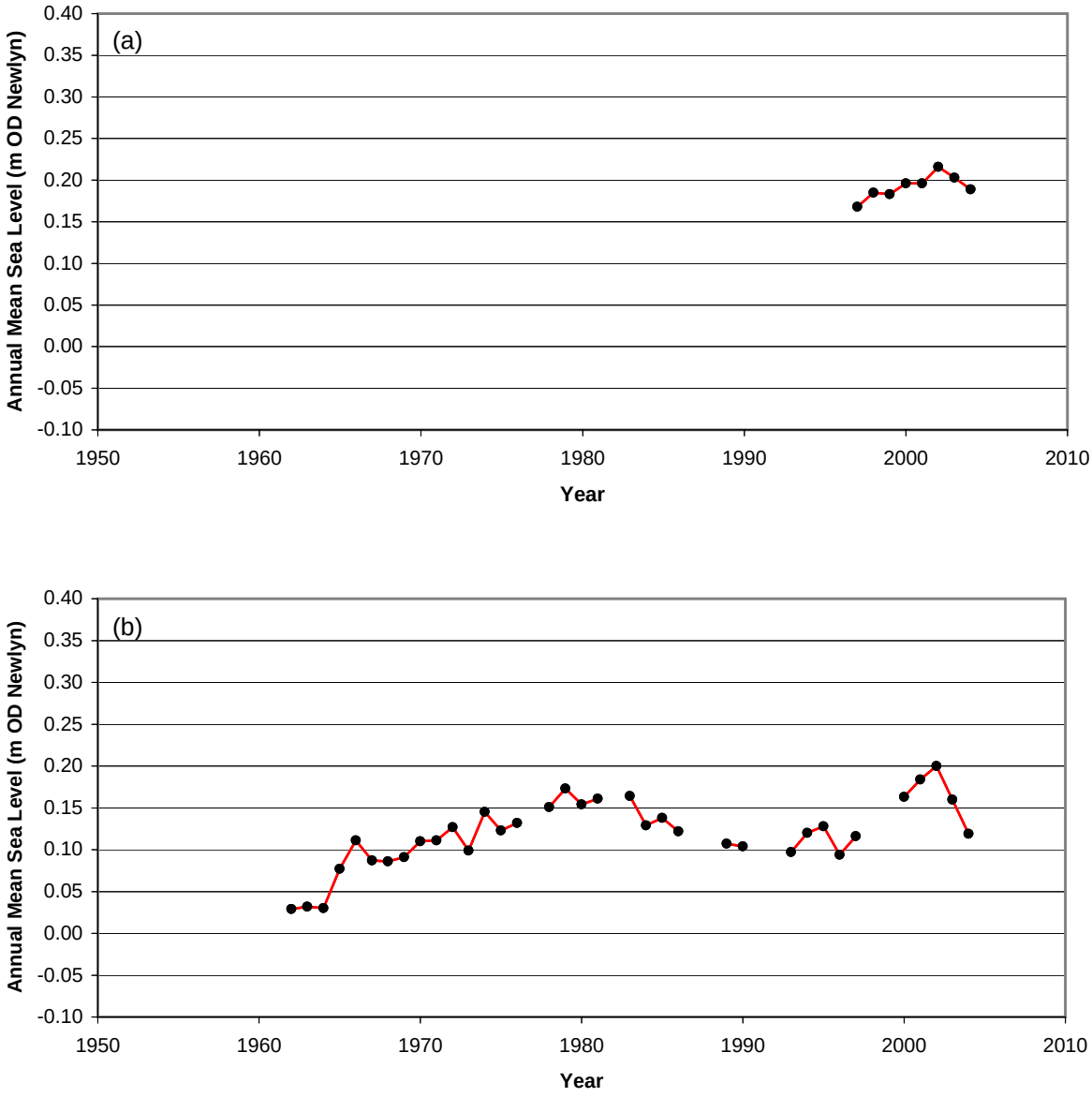

Figure 5.38 Annual mean sea level recorded at (a) Bournemouth and (b) Portsmouth. Data source: Permanent Service for Mean Sea Level.

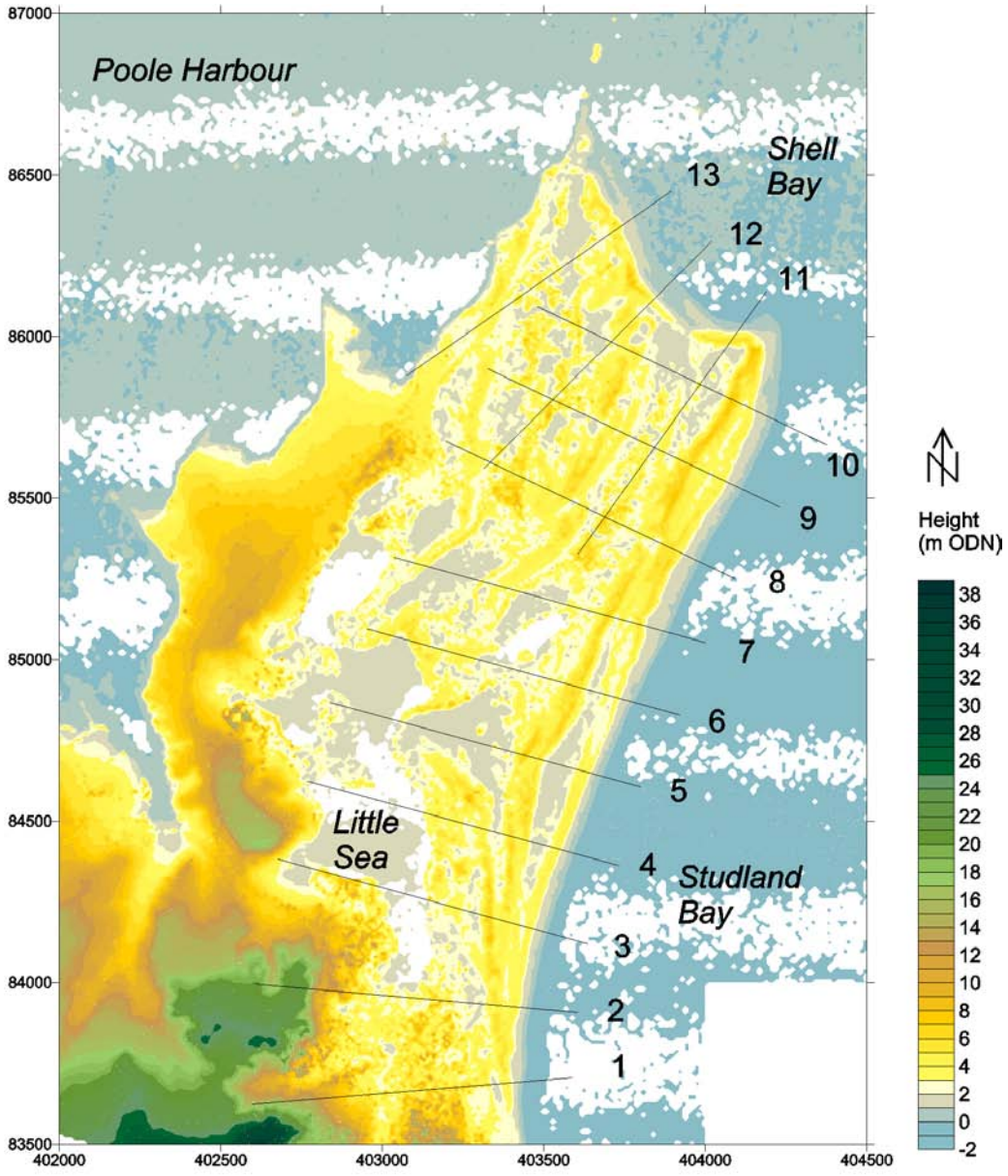

Figure 5.39 Digital terrain model of Studland Bay obtained from lidar data flown in March 1998.

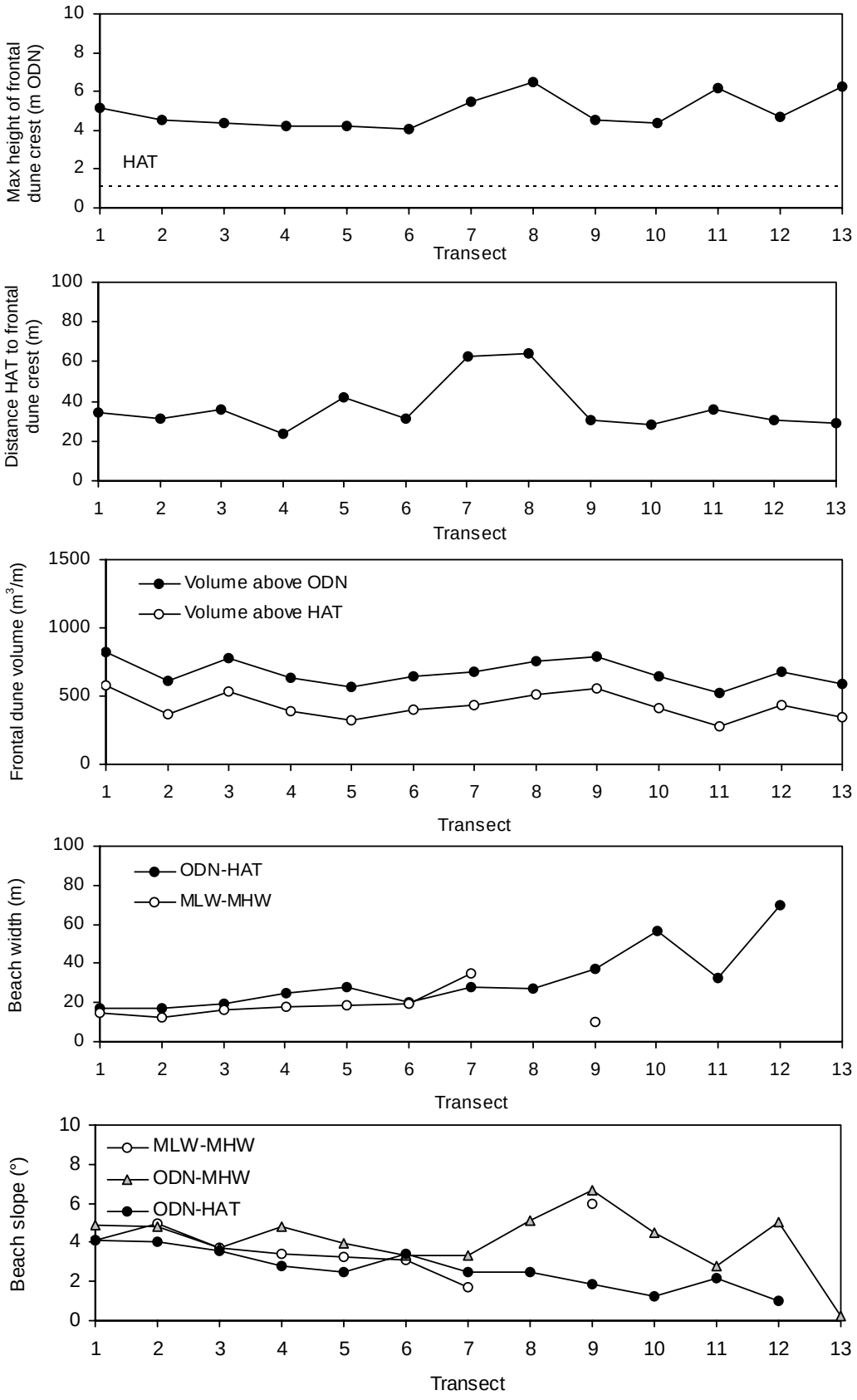

Figure 5.40 Longshore variation in beach and dune morphometric parameters derived from lidar data, Studland Bay. Transect positions are shown on Figure 5.39.

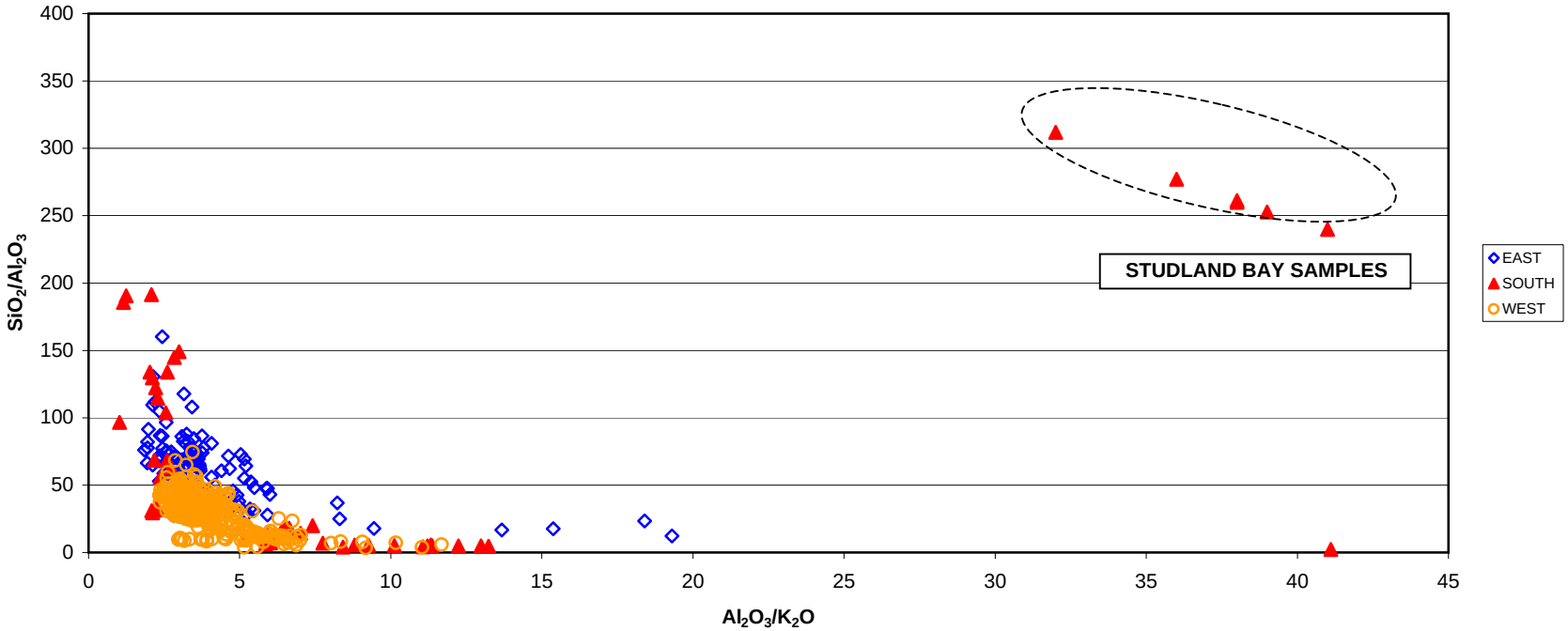

Figure 5.41 Bivariate plots of the aluminium oxide:potassium oxide ratio versus the silica:aluminium oxide ratio for the 63-250 µm grain size fraction of dune samples from locations on the east, south and west coasts of England and Wales, showing the anomalous character of the Studland Bay samples.

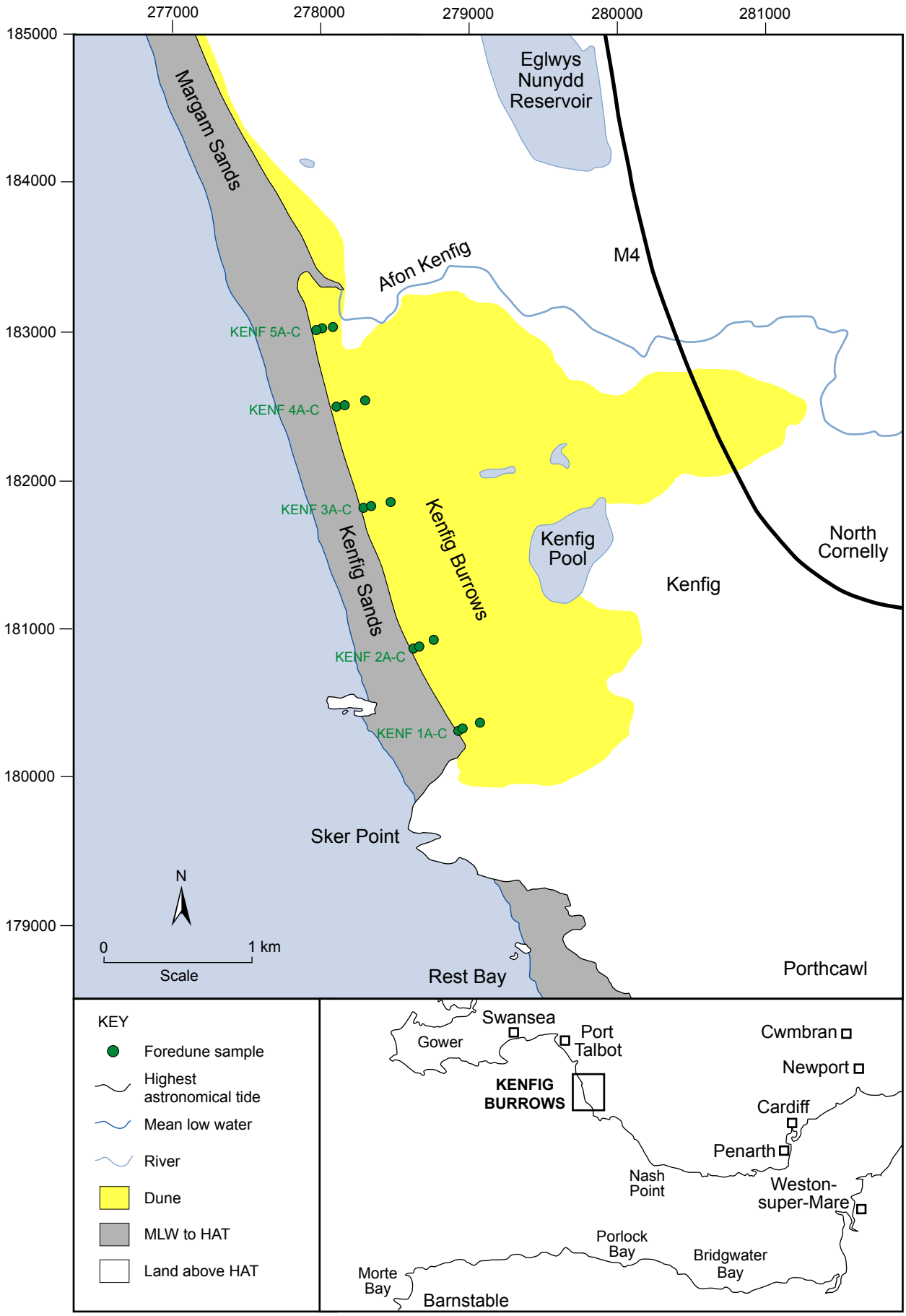

Figure 5.42 The main physical features of Kenfig Burrows, showing dune sediment sampling locations.

Figure 5.43 Aerial photograph of Kenfig Burrows, taken *c*. 1999. The dark area in the centre is Kenfig Pool. Source: Google Earth.

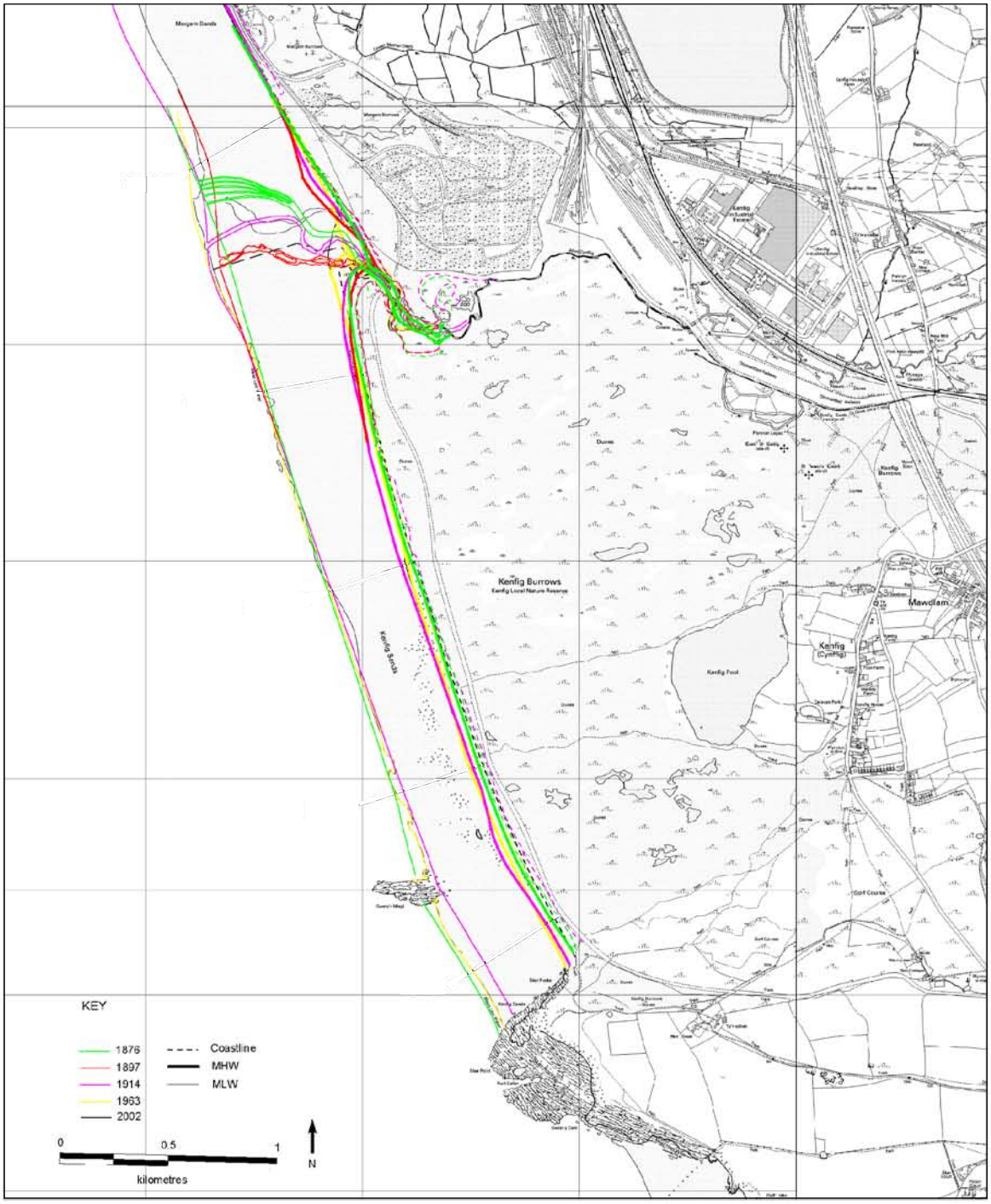

Figure 5.44 Historical changes in the position of the coastline at Kenfig Burrows based on Ordnance Survey maps surveyed in 1876, 1897, 1914, 1963 and 2002. Source: Pye and Saye (2005).

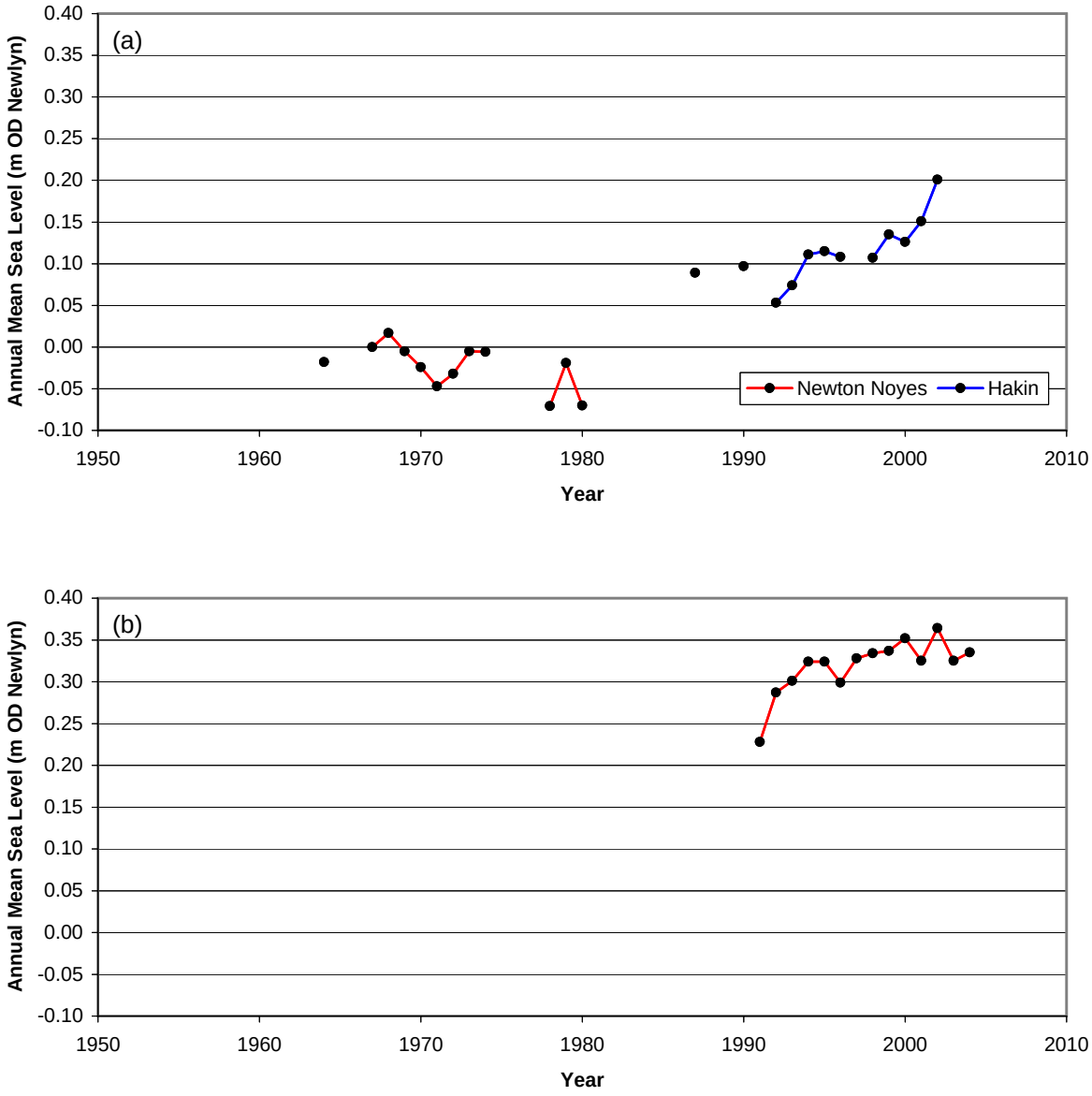

Figure 5.45 Annual mean sea level recorded at: (a) Milford Haven (Newton Noyes and Hakin); and (b) Hinkley Point. Data source: Permanent Service for Mean Sea Level.

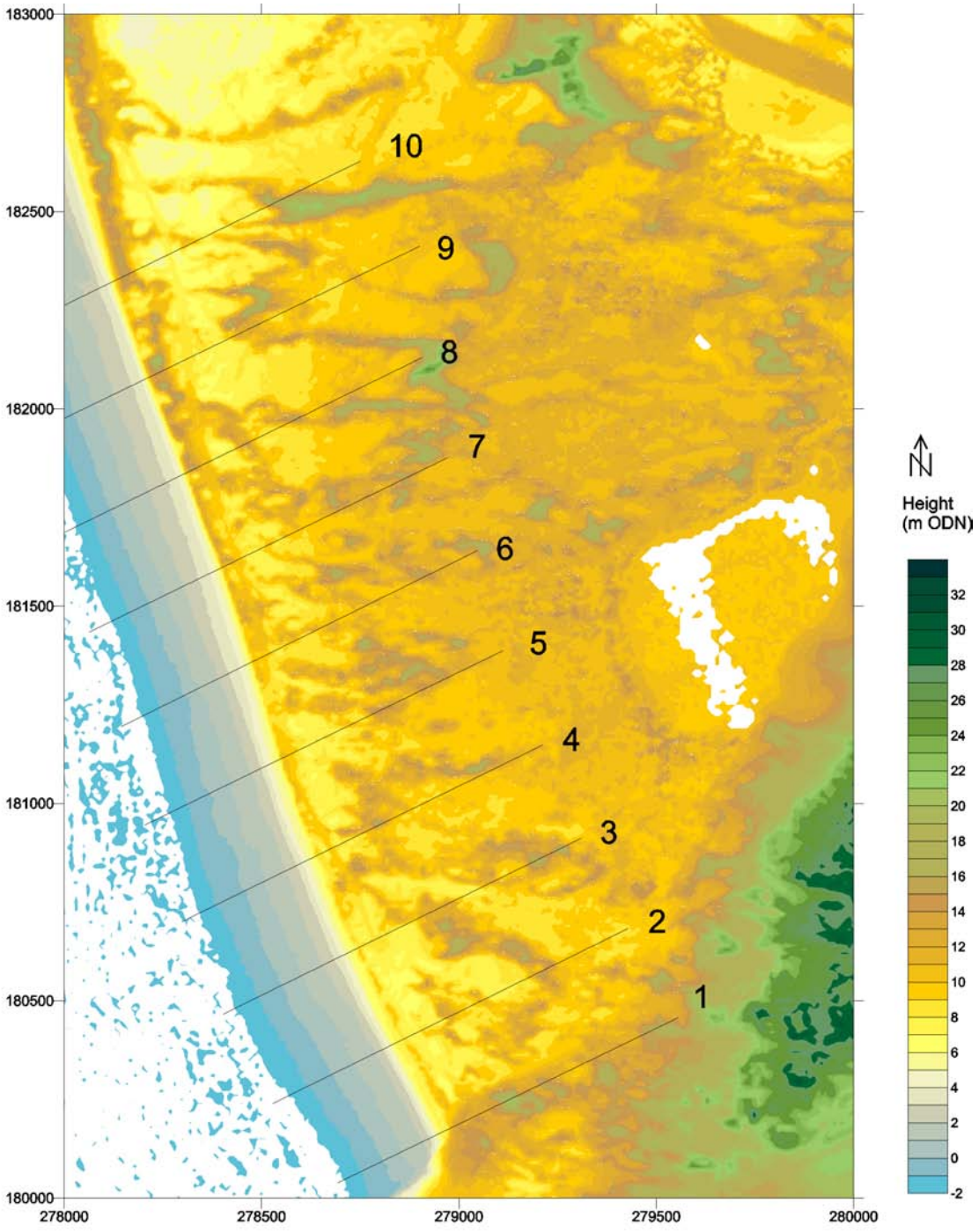

Figure 5.46 Digital terrain model of Kenfig Burrows obtained from lidar data flown in November 1999.

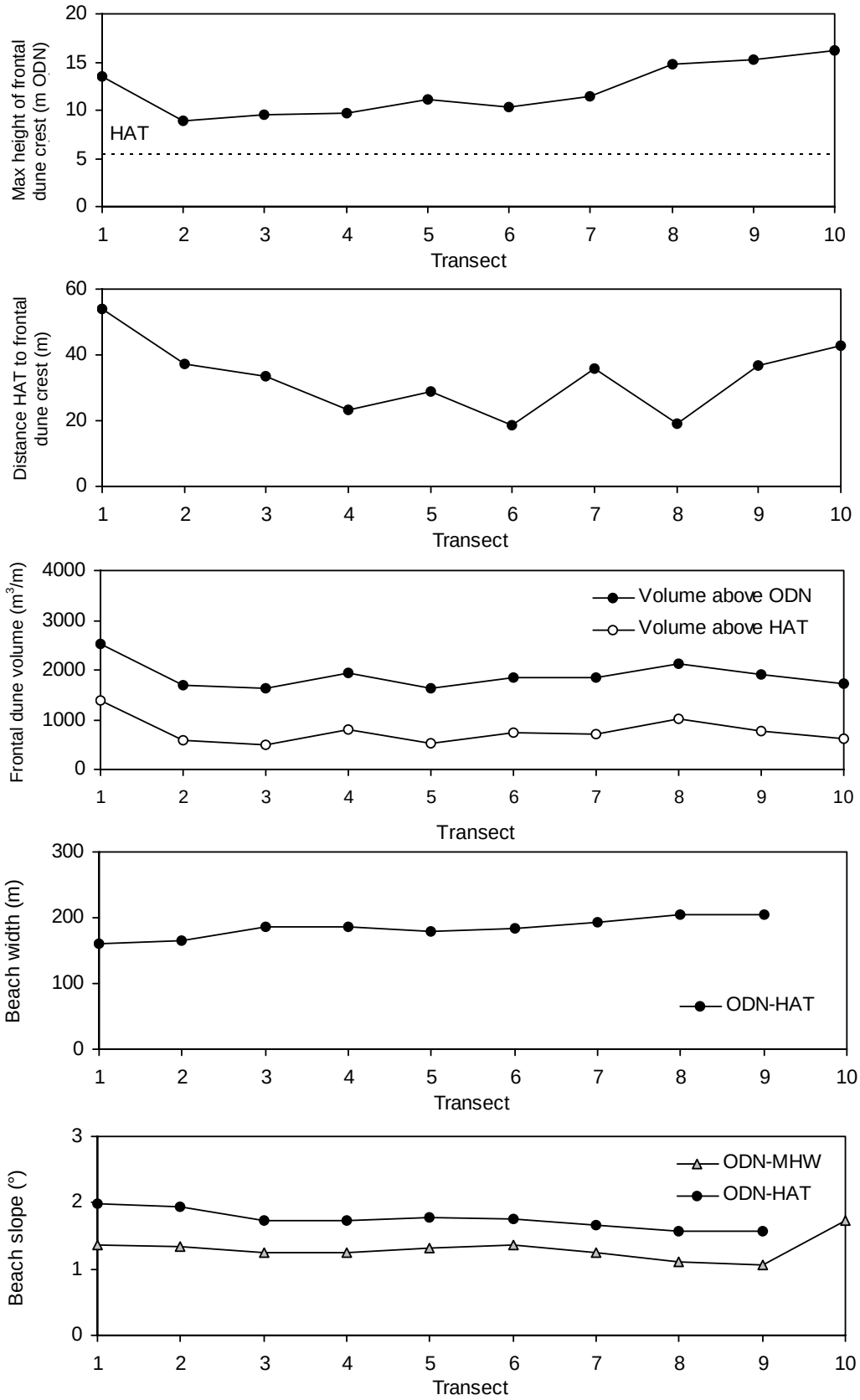

Figure 5.47 Longshore variation in beach and dune morphometric parameters derived from lidar data, Kenfig Burrows. Transect positions are shown on Figure 5.46.

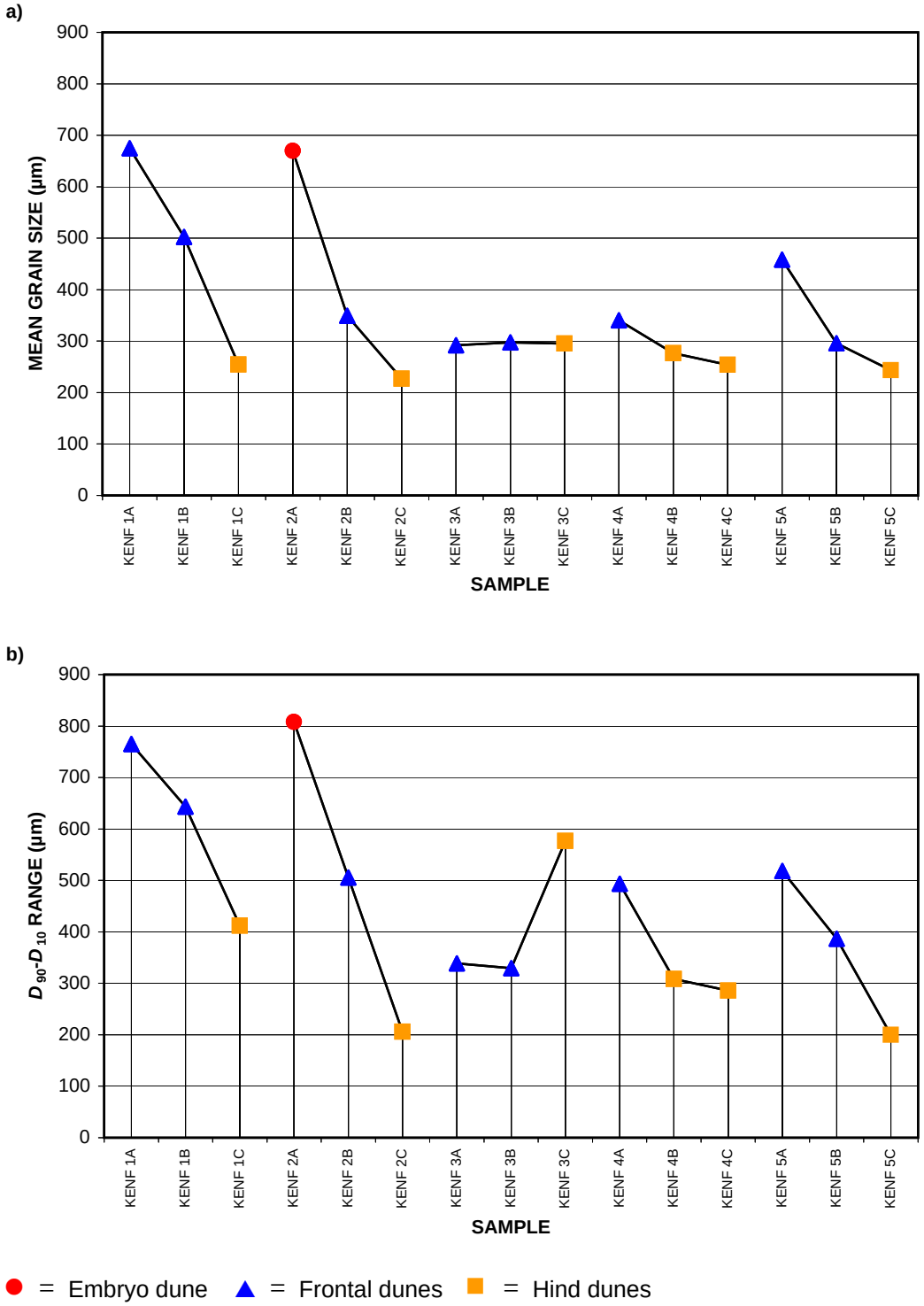

Figure 5.48 Variation in a) mean grain size and b) sorting of dune sand samples collected along transects at Kenfig Burrows. Transects are linked and ordered from south to north (see Figure 5.42 for locations)

Plates

Plate 5.1 Accreting foredunes at Ainsdale south, Sefton coast, looking north.

Plate 5.2 Advancing 'nose' of dune downwind of Devil's Hole Blowout, Ravenmeols, Sefton Coast.

Plate 5.3 Cliff-fall in nicotine dump spoil, frontal dunes near Kirklake Path, Formby.

Plate 5.4 Holocene silts exposed on foreshore by coastal erosion north of Kirklake Path, Formby.

Plate 5.5 Recent sand accretion in front of the promenade, north of Seaforth container terminal, looking north.

Plate 5.6 Eroding frontal dunes near Victoria Road, Freshfield, looking north.

Plate 5.7 Ad hoc protection formed by rubble dumping, northern end of Spurn Peninsula, looking north.

Plate 5.8 Low, narrow dune ridge at the northern end of Spurn Peninsula, looking north.

Plate 5.9 Eroding dunes on a section of shore partially protected by degraded groynes, wooden revetments and concrete walls, north-central part of the Spurn Peninsula, view looking south.

Plate 5.10 Accreting embryo dunes near Chalk Bank Hide, south central part of Spurn Peninsula, looking south.

Plate 5.11 Stable dune frontage near the lighthouse, southern end of Spurn Peninsula, looking southwards. Note the World War II pill box on the beach.

Plate 5.12 Dunes on the estuary side of the Spurn Peninsula, near the lifeboat station, looking south.

Plate 5.13 Armourstone protection around golf clubhouse salient, Brancaster Bay, looking west.

Plate 5.14 The eroding dune frontage at Brancaster during the 1930s. Source: Steers (1935).

Plate 5.15 Unprotected low foredune ridge, western part of Brancaster Bay, looking west.

Plate 5.16 A low, slowly eroding foredune ridge and back-barrier marsh near Titchwell, Brancaster Bay, looking west.

Plate 5.17 Sand-trapping structures at the foredune toe, east of the golf clubhouse, Brancaster Bay, looking east. Note also the relict groynes on the foreshore.

Plate 5.18 Eroded foredune protected by gabion revetment, west of Brancaster golf clubhouse, looking WSW.

Plate 5.19 Ad hoc protection using rubble and bags filled with stones, plus chestnut palings, west of Brancaster golf clubhouse, looking west.

Plate 5.20 Close-up of sand-trapping sturctures, eastern part of Brancaster Bay, looking west.

Plate 5.21 Stable/slowly accreting foredunes on central part of Studland Bay, looking south.

Plate 5.22 Accreting foredunes at the northern end of Studland Bay, looking SSW.

Plate 5.23 Accreting hummock dunes near the ferry crossing at the northern end of South Haven (Studland) Peninsula, looking north-east towards Sandbanks with Poole Harbour to the left.

Plate 5.24 View looking NNW along the frontal dunes at Kenfig Burrows.

Plate 5.25 Eroding section of frontal dune at Kenfig Burrows, fronted by a mixed sand-gravel upper beach.

Plate 5.26 Eroded, hummocky dune topography, central Kenfig Burrows.

Plate 5.27 Artificially deepened blowout in the first dune ridge behind the frontal dunes at Kenfig Burrows, looking ENE.

Plate 5.28 Shingle ridge in front of a cliffed frontal dune, near the northern end of Kenfig Burrows.

PB 12527 / 24

Nobel House
17 Smith Square
London SW1P 3JR

www.defra.gov.uk